Journal of the American Heart Association

ORIGINAL RESEARCH

Validation of Specific and Reliable Genetic Tools to Identify, Label, and Target Cardiac Pericytes in Mice

Linda Alex, PhD; Izabela Tuleta, MD, PhD; Venugopal Harikrishnan, PhD; Nikolaos G. Frangogiannis, MD

BACKGROUND: In the myocardium, pericytes are often confused with other interstitial cell types, such as fibroblasts. The lack of well-characterized and specific tools for identification, lineage tracing, and conditional targeting of myocardial pericytes has hampered studies on their role in heart disease. In the current study, we characterize and validate specific and reliable strategies for labeling and targeting of cardiac pericytes.

METHODS AND RESULTS: Using the neuron-glial antigen 2 (NG2)^{DsRed} reporter line, we identified a large population of NG2+ periendothelial cells in mouse atria, ventricles, and valves. To examine possible overlap of NG2+ mural cells with fibroblasts, we generated NG2^{DsRed}; platelet-derived growth factor receptor (PDGFR) α^{EGFP} pericyte/fibroblast dual reporter mice. Myocardial NG2+ pericytes and PDGFRα+ fibroblasts were identified as nonoverlapping cellular populations with distinct transcriptional signatures. PDGFRα+ fibroblasts expressed high levels of fibrillar collagens, matrix metalloproteinases, tissue inhibitor of metalloproteinases, and genes encoding matricellular proteins, whereas NG2+ pericytes expressed high levels of *Pdgfrb*, *Adamts1*, and *Vtn*. To validate the specificity of pericyte Cre drivers, we crossed these lines with PDGFRα^{EGFP} fibroblast reporter mice. The constitutive NG2^{Cre} driver did not specifically track mural cells, labeling many cardiomyocytes. However, the inducible NG2^{CreER} driver specifically traced vascular mural cells in the ventricle and in the aorta, without significant labeling of PDGFRα+ fibroblasts. In contrast, the inducible PDGFRβ^{CreER} line labeled not only mural cells but also the majority of cardiac and aortic fibroblasts.

CONCLUSIONS: Fibroblasts and pericytes are topographically and transcriptomically distinct populations of cardiac interstitial cells. The inducible NG2^{CreER} driver optimally targets cardiac pericytes; in contrast, the inducible PDGFRβ^{CreER} line lacks specificity.

Key Words: aorta ■ fibroblast ■ lineage tracing ■ myocardium ■ pericyte

Blood vessels are composed of 2 distinct cell types: an inner layer of endothelial cells and mural cells that coat the endothelial cell tube. Mural cells can be further subdivided into vascular smooth muscle cells (VSMCs) and pericytes. VSMCs are associated with larger conduit vessels (such as arteries and veins), whereas pericytes enwrap the small caliber capillaries and are embedded within the endothelial basement membrane.[1–3] Pericytes are ubiquitously present in microvessels of all tissues, represent a critical interface between the circulating blood and the interstitium,[3,4] and have been implicated in both physiologic functions and pathophysiologic responses. Contractile pericytes contribute to the regulation of blood flow in the brain[5] and the kidney,[6] regulating basal blood flow resistance,[7,8] and have been implicated in blood pressure control.[9] Cerebral pericytes play a central role in the development and preservation of the blood-brain-barrier[10,11] and regulate vascular immune homeostasis in the central nervous system.[12] Pericytes may also be

Correspondence to: Nikolaos G. Frangogiannis, MD, The Wilf Family Cardiovascular Research Institute, Albert Einstein College of Medicine, 1300 Morris Park Avenue Forchheimer G46B, Bronx NY 10461. E-mail: nikolaos.frangogiannis@einsteinmed.org

Supplementary Material for this article is available at https://www.ahajournals.org/doi/suppl/10.1161/JAHA.121.023171

For Sources of Funding and Disclosures, see page 15.

JAHA is available at: www.ahajournals.org/journal/jaha

CLINICAL PERSPECTIVE

What Is New?

- We characterized mouse cardiac pericytes and demonstrated that myocardial neuron-glial antigen 2 (NG2)+ pericytes and platelet-derived growth factor receptor (PDGFR)α+ fibroblasts are nonoverlapping interstitial cell populations with distinct transcriptomic profiles.
- We documented that the inducible NG2^{CreER} mouse line optimally targets cardiac pericytes; in contrast, the germline NG2-Cre mice and the inducible PDGFRβ-Cre driver lack specificity.

What Are the Clinical Implications?

- Our characterization and validation of genetic tools for labeling, tracing and targeting cardiac pericytes will greatly facilitate experimental investigations exploring the role of this understudied cell type in heart disease.

Nonstandard Abbreviations and Acronyms

α-SMA	α smooth muscle actin
CreER™	tamoxifen-inducible Cre recombinase
Dsred	Discosoma species red
EGFP	enhanced green fluorescent protein
NG2	neuron-glial antigen 2
PCR	polymerase chain reaction
PDGFR	platelet-derived growth factor receptor
tdTomato	tandem dimer Tomato
VSMC	vascular smooth muscle cell

implicated in a wide range of pathologic responses, including inflammation,[13] fibrosis,[14–16] and neoplasia.[17,18]

In the adult mammalian heart, maintenance of normal function and preservation of chamber geometry are not only dependent on contractile cardiomyocytes but also require the contribution of several other cell types, including macrophages, fibroblasts, and vascular cells. The myocardium contains a rich network of vessels necessary to provide perfusion in order to meet the high metabolic needs of cardiomyocytes. Considering the abundance of cardiac microvessels, it is not surprising that adult mammalian hearts contain a large population of pericytes.[19–24] Through their interactions with vascular endothelial cells, myocardial pericytes can regulate perfusion and vascular permeability. Moreover, in myocardial diseases, pericytes may contribute to the regulation of inflammatory, fibrogenic, and angiogenic responses. Despite their abundance and the diverse range of their functional properties, myocardial pericytes remain poorly understood. Most of the evidence implicating pericytes in cardiac pathophysiology is based on associative data. Studies in cells harvested from patients with heart failure have demonstrated that pericytes from cardiomyopathic hearts exhibit impaired mechanotransduction.[25] Moreover, animal model studies have suggested that pericytes may play a role in early postischemic microvascular injury,[26] may be involved in "no-reflow" following ischemia and reperfusion,[27,28] and may contribute to the pathogenesis of the cardiomyopathy associated with receptor tyrosine kinase inhibitor treatment.[29] However, investigations documenting the involvement of pericytes in myocardial diseases using genetic approaches are lacking. Understanding the role of pericytes in heart disease is hampered by the absence of well-characterized, specific, and reliable approaches for labeling and cell-specific targeting of pericytes in vivo. A major source of confusion is the abundance of cardiac fibroblasts,[30] cells of mesenchymal origin that can be located in close proximity to vessels and may exhibit profiles that overlap with those of pericytes. Thus, study of the role of pericytes in myocardial disease requires validation and characterization of reporter lines and Cre drivers with specificity for pericytes and with no significant overlap with fibroblasts.

Published evidence on the molecular tools used for pericyte-specific targeting generates confusion. Although the platelet-derived growth factor receptor (PDGFR)β was found to be exclusively expressed in pericytes in the brain,[31] its specificity as a pericyte marker in other organs is controversial. Inducible PDGFRβ-Cre lines were used for pericyte-specific targeting in some studies[32,33] and for fibroblast-specific targeting in other investigations.[34,35] The proteoglycan neuron-glial antigen 2 (NG2) is a commonly used pericyte marker[36]; however, the specificity and reliability of constitutive and inducible NG2-Cre lines in targeting myocardial pericytes have not been studied. In the current investigation, we validated and characterized genetic tools for pericyte-specific labeling and targeting. Using dual reporter mice, we identified phenotypically and transcriptomically distinct pericyte and fibroblast populations in the adult mouse heart. To study the reliability of pericyte-specific Cre drivers, we used a fibroblast reporter system. Our findings suggest that inducible NG2-Cre lines specifically target cardiac mural cells. In contrast, inducible PDGFRβ-Cre drivers lack specificity, exhibiting recombination in both mural cells and the majority of interstitial fibroblasts.

METHODS

The data that support the findings of this study are available from the corresponding author upon reasonable request.

Mice

All animal experiments were performed according to the animal experimental guidelines issued by the Animal Care and Use Committee at Albert Einstein College of Medicine and conform to the *Guide for the Care and Use of Laboratory Animals* published by the National Institutes of Health. $NG2^{DsRed/+}$, constitutively active NG2-Cre ($NG2^{Cre/+}$), tamoxifen-inducible NG2 Cre recombinase ($NG2^{iCre/+}$), tamoxifen-inducible PDGFRβ-$CreER^{T2}$ ($PDGFR\beta^{iCre/+}$), reverse orientation splice acceptor (ROSA) $26^{tdTomato-/-}$ ($R26^{tdTomato}$), $ROSA26^{EYFP-/-}$ ($R26^{EYFP}$), $PDGFR\alpha^{EGFP/+}$ mice were purchased from Jackson Laboratories (Table). $NG2^{DsRed}$;$PDGFR\alpha^{EGFP}$ double reporter mice were generated by breeding $NG2^{DsRed/+}$ mice with $PDGFR\alpha^{EGFP/+}$. Both male and female 2- to 3-month-old mice were euthanized for histological end points and fluorescence-activated cell sorting studies. $NG2^{Cre/+}$ mice were crossed with $R26^{EYFP}$ mice to develop $NG2^{Cre/+}$;$R26^{EYFP}$ mice. $NG2^{iCre/+}$ or $PDGFR\beta^{iCre/+}$ mice bred into $R26^{tdTomato}$ background were further crossed with $PDGFR\alpha^{EGFP}$ fibroblast reporter mice to enable the simultaneous identification of mural cell–derived progeny, as well as fibroblasts. For lineage tracing studies, 10- to 12-week-old $NG2^{iCre/+}$;$R26^{tdTomato}$;$PDGFR\alpha^{EGFP}$ and $PDGFR\beta^{iCre/+}$;$R26^{tdTomato}$;$PDGFR\alpha^{EGFP/+}$ mice received intraperitoneal injections of tamoxifen (Sigma-T5648, CAS#10540-29-1) at a dosage of 100 mg/kg administered over a course of 5 consecutive days once every 24 hours. Mice were euthanized for histology 2 days after the last injection of tamoxifen.

Immunohistochemistry

For histopathological analysis, mice were euthanized and hearts were fixed in Z-fix (Anatech) and embedded in paraffin. Sequential 5-μm sections were cut from base to apex at 250-μm intervals. Following citrate buffer-mediated antigen retrieval, sections were allowed to cool for close to an hour and then blocked with Tris-buffered saline+0.1% Triton X containing 10% donkey serum. The following antibodies were used: mouse anti-α-smooth muscle actin antibody (dilution 1:100, Sigma F3777), rat anti-Mac-2 antibody (dilution 1:100, Cedarlane Laboratories), goat anti-tdTomato antibody (dilution 1:300, Biorbyt orb334992), rabbit anti-GFP antibody (dilution 1:100, D5.1-2956, Cell Signaling Technology), rabbit anti-CD31 (dilution 1:100, Cell Signaling Technology 89C2, 3528), and rabbit anti-PDGFRβ antibody (1:50, ab32570). Primary antibody incubations were all performed at 4 °C overnight. Following washes in Tris-buffered saline, secondary antibodies raised in donkey were used for 1 hour at room temperature. Sections were washed and then incubated with Trueblack (Biotium 23007) for 20 seconds to quench autofluorescence and then sealed with Fluoro-Gel II mounting medium containing 4',6'-diamidino-2-phenylindole (EMS #17985-50). Slides were then scanned using Zen 3.0 Pro software and a Zeiss Imager M2 microscope (Carl Zeiss Microscopy). Appropriate negative controls using isotype-matched IgG were performed and confirmed the specificity of the immunofluorescence experiments (Figures S1 and S2).

Table. Mouse Lines Used in the Study

	Jackson strain number
$NG2^{DsRed/+}$	008241
$NG2^{Cre/+}$	008533
$NG2^{iCre/+}$	008538
$PDGFR\beta^{iCre/+}$	030201
$ROSA26^{tdTomato-/-}$	007914
$ROSA26^{EYFP-/-}$	006148
$PDGFR\alpha^{EGFP/+}$	007669

EGFP indicates enhanced green fluorescent protein; EYFP, enhanced yellow fluorescent protein; NG2, neuron-glial antigen 2; PDGFR, platelet-derived growth factor receptor; ROSA, reverse orientation splice acceptor; and tdTomato, tandem dimer Tomato.

Quantitative Analysis of Cell Density

Using default algorithms of the Intellesis Trainable Segmentation module of Zen 3.0 Pro software, an artificial intelligence–based model was trained on images representing atria, ventricles, valves, and the ascending aorta (in total, at least 4 images up to 8 images depending on the specific staining used) to identify and count mural cell profiles. Using the Image Analysis module, specific settings were incorporated in the trained model to count the segmented objects. For quantitative analysis, 5 to 10 fields were scanned from 2 to 3 different sections from each chamber under a magnification of 200×. Quantification of cell density was performed separately for the atria, ventricles, valves, and ascending aorta. The data were presented as the number of positive profiles per millimeters squared.

To assess the percentage of arteriolar and aortic medial α smooth muscle actin (α-SMA)+ VSMCs expressing NG2, the number of double positive cells was counted in 4 to 7 fields (400× magnification) from a single level for each mouse using the count tool from Adobe Photoshop. To assess the extent of fibroblast labeling with the PDGFRβ tamoxifen-inducible Cre recombinase ($CreER^{TM}$) driver, we quantitatively assessed the percentage of PDGFRα+ fibroblasts that were labeled with the inducible PDGFRβ-Cre in the ventricular myocardium as well as in the adventitia of the ascending aorta. A total of 8 to 12 fields were analyzed from the ventricular myocardium of each mouse, and 4 to 6 fields were analyzed from the ascending aorta of each mouse (400× magnification). Cells were counted using the count tool from Adobe Photoshop.

Fluorescence-Activated Cell Sorting of Cardiac Pericytes and Fibroblasts

Single-cell suspension for flow cytometry was prepared using a modified version of a previously described protocol.[17] Briefly, atria were removed from the myocardial tissue, and the ventricles were finely minced and suspended in digestion buffer cocktail of collagenase IV (2 mg/mL, Worthington Biochem) and dispase II (1.2 U/mL, Stemcell Technologies) in Dulbecco phosphate-buffered saline. Tissue fragments were then incubated at 37 °C for 15 minutes with gentle rocking. After incubation, a tissue digestion buffer with tissue clusters was triturated by pipetting 10 times using a 10-mL serological pipette. Tissue fragments were again incubated at 37 °C and triturated twice more (45 minutes of total digestion time). The final trituration was conducted by pipetting 30× with a p1000 pipette. Cell suspension was filtered through a 40-µm cell strainer into 50-mL tubes containing 40 mL of Dulbecco phosphate-buffered saline and centrifuged for 20 minutes at 200*g* with centrifuge brakes deactivated to remove cell debris. Cells were then resuspended in 1× Red Blood Cell Lysis Buffer (eBioscience) and incubated for 5 minutes at room temperature. Cell suspension was then centrifuged at 500*g* for 5 minutes at room temperature and resuspended in Hanks Balanced Salt Solution containing 2% fetal bovine serum. Cells in single-cell suspensions were blocked with anti-mouse CD16/CD32 (1:250, BD Biosciences) for 30 minutes at 4 °C. To identify hematopoietic and endothelial cells, the cell suspension was incubated for 1 hour at 4 °C with anti-CD31-BV605 (1:100, BioLegend) and anti-CD45-APC-Cy7 (2.5:100, BioLegend). Cell suspension was washed and labeled with calcein violet 450 (1.25 µmol/L, eBioscience, Invitrogen) to identify metabolically active cells and 7-aminoactinomycin D (1:500, Invitrogen) to identify cells with compromised cell membranes. Nonhematopoietic/nonendothelial cells (CD45–/CD31–) were gated to identify $NG2^{RFP}$+ pericytes and $PDGFR\alpha^{EGFP}$+ fibroblasts, which were sorted with a FACSAria Sorter (BD Biosciences). FlowJo software (BD) was used for data analysis. The gating strategy and controls for each marker using $NG2^{DsRed}$ and $PDGFR\alpha^{EGFP}$ single reporter mice are shown in Figure S3.

RNA Isolation and Polymerase Chain Reaction Array

RNA isolation of sorted cells was performed using Dynabeads mRNA Direct Kit (61012, Invitrogen). Following isolation, RNA was converted to cDNA using a Qiagen RT2 First Strand Kit (330404). Quantitative polymerase chain reaction (PCR) was performed using the mouse RT2 Profiler extracellular matrix PCR array according to manufacturer's protocol (PAMM-013Z, Qiagen). Separately, quantitative PCR was also performed for the mural cell genes *Pdgfrb* (forward: 5' CACCTTCTCCAGTGTGCTGA 3', reverse: 5' GGAGTCCATAGGGAGGAAGC 3') and *Acta2* (forward: 5' GAGTAATGGTTGGAATGG 3', reverse: 5' ATGATGCCGTGTTCTATC 3'). Primers were synthesized by Integrated DNA Technologies. The same thermal profile conditions were used for all primer sets: 95 °C for 10 minutes, 40 cycles at 95 °C for 15 seconds, and 60 °C for 1 minute on the CFX384™ Real-Time PCR Detection System (Bio-Rad). The data obtained were analyzed using the ΔCt method.

Statistical Analysis

For comparisons of 2 groups, an unpaired 2-tailed Student *t* test using (when appropriate) Welch correction for unequal variances was performed. Mann-Whitney test was used for comparisons between 2 groups that did not show Gaussian distribution. For comparisons of multiple groups, 1-way ANOVA was performed followed by Sidak multiple comparison test for normal distributions or the Kruskal-Wallis test for non-Gaussian distributions. Data are expressed as mean±SE. Statistical significance was set at 0.05.

RESULTS

Adult Mouse Heart Contains a Large Population of Periendothelial NG2+ Cells

To identify pericytes in the adult mouse myocardium, we used the $NG2^{DsRed/+}$ reporter line. Dual immunofluorescence for $NG2^{RFP}$ and the endothelial cell marker CD31 identified a large population of myocardial NG2+ cells, located in close proximity to endothelial cells (Figure 1A). Quantitative analysis showed that the ventricles contained more NG2+ cells than the atria (Figure 1B). Significant numbers of NG2+ cells were also noted in the valve leaflets (Figure 1C). The aortic valve had a higher density of NG2+ cells than the mitral and tricuspid valves (Figure 1D).

NG2 Labels a Subset of Arteriolar and Aortic VSMCs

Next, we examined the sensitivity of NG2 in the labeling of VSMCs, using dual fluorescence for NG2 and α-SMA (Figure 2). In the myocardium, α-SMA labeled only arteriolar VSMCs without staining NG2+ microvascular pericytes (Figure 2A and 2B). Two distinct populations of cardiac arteriolar VSMCs were identified on the basis of NG2 fluorescence intensity. The majority of arteriolar VSMCs (91.49%±3.02%, n=8) had high levels of NG2 expression, whereas a much smaller subpopulation (8.51%±3.02%, n=8) exhibited low NG2 expression levels (Figure 2A and 2B). In the mouse myocardium, NG2+/α-SMA– cells (representing microvascular pericytes) were much more abundant than arteriolar NG2+/α-SMA+ VSMCs

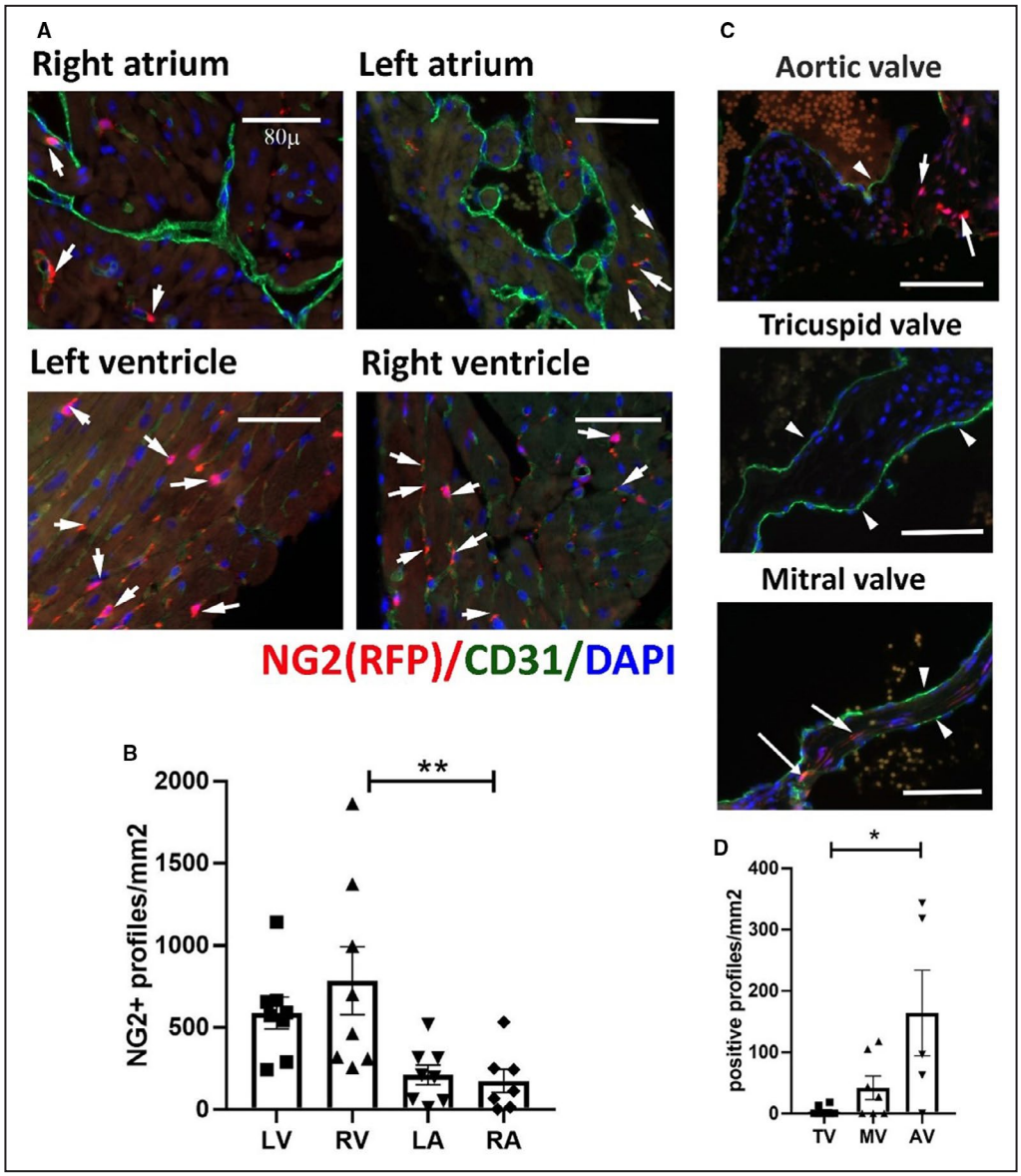

Figure 1. The neuron-glial antigen 2 (NG2)^{DsRed} reporter model identifies a large population of pericytes in the mouse myocardium.
A, Dual immunofluorescence for red fluorescent protein (RFP) and CD31 identifies NG2+ pericytes in atria and ventricles (arrows), associated with CD31+ endothelial cells (**A**). **B**, Quantitative analysis shows that the density of pericytes is higher in the right ventricle (RV) than in the right atrium (RA). Moreover, there is a trend (P=0.08) toward a higher pericyte density in the left ventricle (LV), in comparison to the left atrium (LA). **C**, Dual immunofluorescence identifies NG2+ cells (arrows) in the valves. The arrowheads indicate the CD31+ valvular endothelial cells. **D**, The aortic valve (AV) has a higher density of pericytes than the mitral valve (MV) and tricuspid valve (TV) (*P<0.05, **P<0.01; n=5–8 per group). Scalebar=80 μm. Data are expressed as mean±SE. Statistical comparison was performed by ANOVA, followed by the Sidak post hoc test (**B**), or the nonparametric Kruskal-Wallis test (**D**). DAPI indicates 4',6'-diamidino-2-phenylindole; and Dsred, Discosoma species red.

(Figure 2C). In the ascending aorta, only 46.2%±8.0% (n=6) of the α-SMA+ VSMCs in the media were positive for NG2 (Figure 2D through 2F). In the aortic adventitia, NG2 staining identified a significant number of α-SMA– cells that may represent microvascular pericytes coating the vasa vasorum (Figure 2G through 2I).

Myocardial NG2+ Cells Express the Mural Cell Marker PDGFRβ But Not the Fibroblast Marker PDGFRα and the Macrophage Marker Mac2

We next investigated the specificity of NG2 labeling as a mural cell marker. Dual fluorescence for

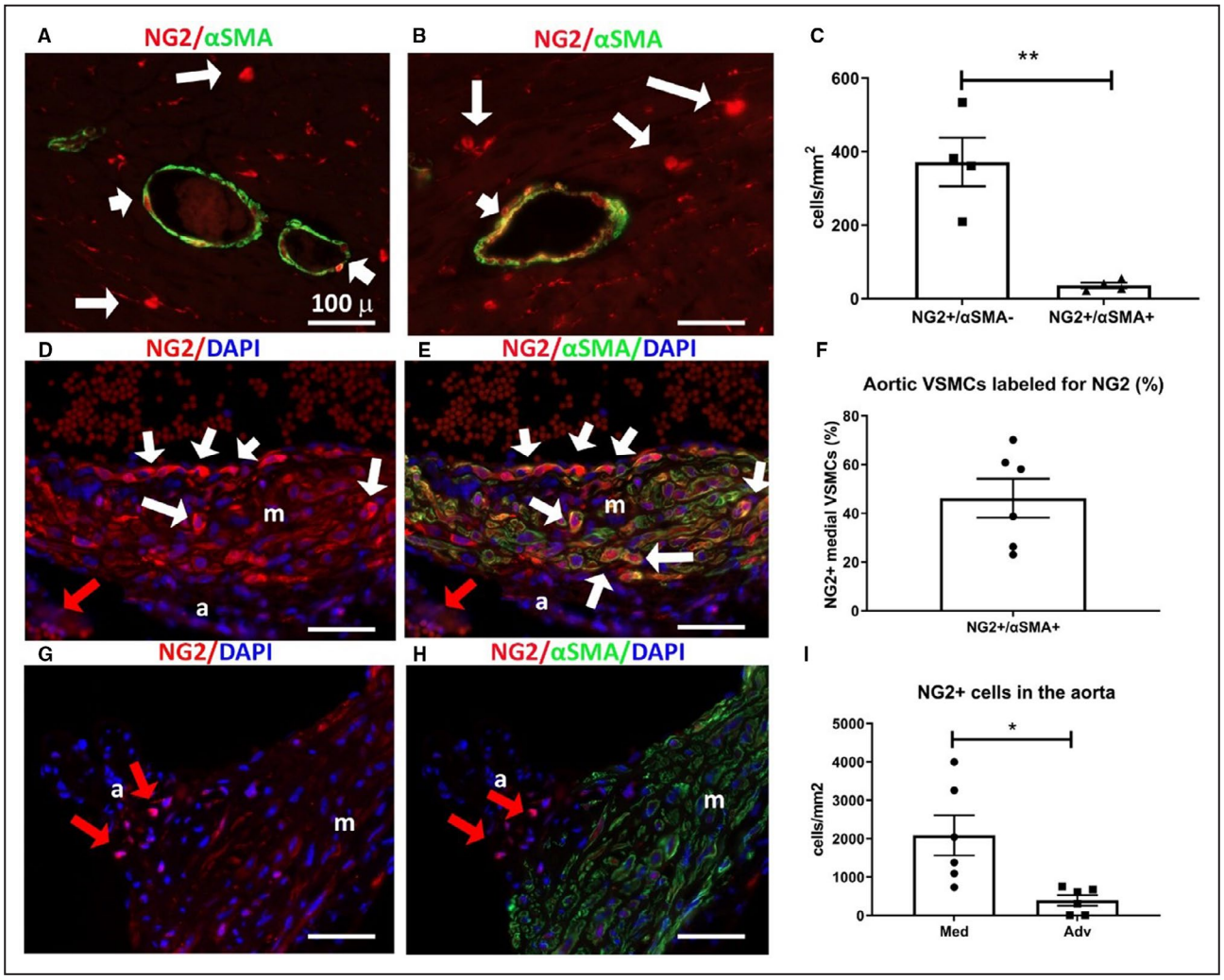

Figure 2. Neuron-glial antigen 2 (NG2) labels a subset of vascular smooth muscle cells (VSMCs) in the myocardial arterioles and the ascending aorta.

A and **B**, Dual fluorescence for red fluorescent protein (RFP) and α-smooth muscle actin (α-SMA) in the $NG2^{DsRed}$ model, identifies a subset of arteriolar α-SMA+ VSMCs that express NG2 (short arrows). However, the majority of NG2+ profiles are α-SMA– microvascular pericytes (long arrows). **C**, Quantitative analysis shows that the density of NG2+/α-SMA– profiles (microvascular pericytes) is much higher than the density of NG2+/α-SMA+ cells (arteriolar VSMCs) (**P<0.01; n=4 per group). **D** through **F**, In the ascending aorta, dual fluorescence for RFP and α-SMA shows ≈40% of aortic VSMCs in the media (m) are NG2+ (long arrows). **G** and **H**, In the aortic adventitia (a), NG2+/α-SMA– profiles (red arrows) represent the pericytes of the aortic vasa vasorum. **I**, The density of NG2+ cells in the aortic media is much higher than the number of adventitial NG2+ cells (*P<0.05; n=6 per group). Scalebar=100 μm. Data are expressed as mean±SE. Statistical comparison was performed using Welch t test. Adv indicates adventitia; DAPI, 4',6'-diamidino-2-phenylindole; Dsred, Discosoma species red; and Med, media.

NG2 and the mural cell marker PDGFRβ showed that the majority of NG2+ cells were also PDGFRβ+ (Figure 3A through 3C). However, a large fraction of cardiac interstitial cells also exhibited PDGFRβ immunoreactivity in the absence of NG2 expression (Figure 3A through 3D). To examine whether a subset of the NG2+ cells were fibroblasts, we generated pericyte/fibroblast ($NG2^{DsRed}$;$PDGFR\alpha^{EGFP}$) dual reporter mice. Dual fluorescence showed that NG2 does not label any PDGFRα+ fibroblasts in the mouse heart (Figure 3E through 3G). To examine whether NG2 may label a subset of macrophages, we performed dual fluorescence for NG2 and the macrophage marker Mac2. The Mac2+ population in the mouse heart was distinct from the NG2-expressing cells (Figure 3H through 3J).

NG2+ Pericytes and PDGFRα+ Fibroblasts Have Distinct Transcriptomic Profiles

To compare the transcriptional signatures of myocardial pericytes and fibroblasts, we extracted RNA from sorted NG2+ and PDGFRα+ cells from adult mouse hearts. There was no significant overlap between these 2 populations (Figure 4A). A PCR array showed that

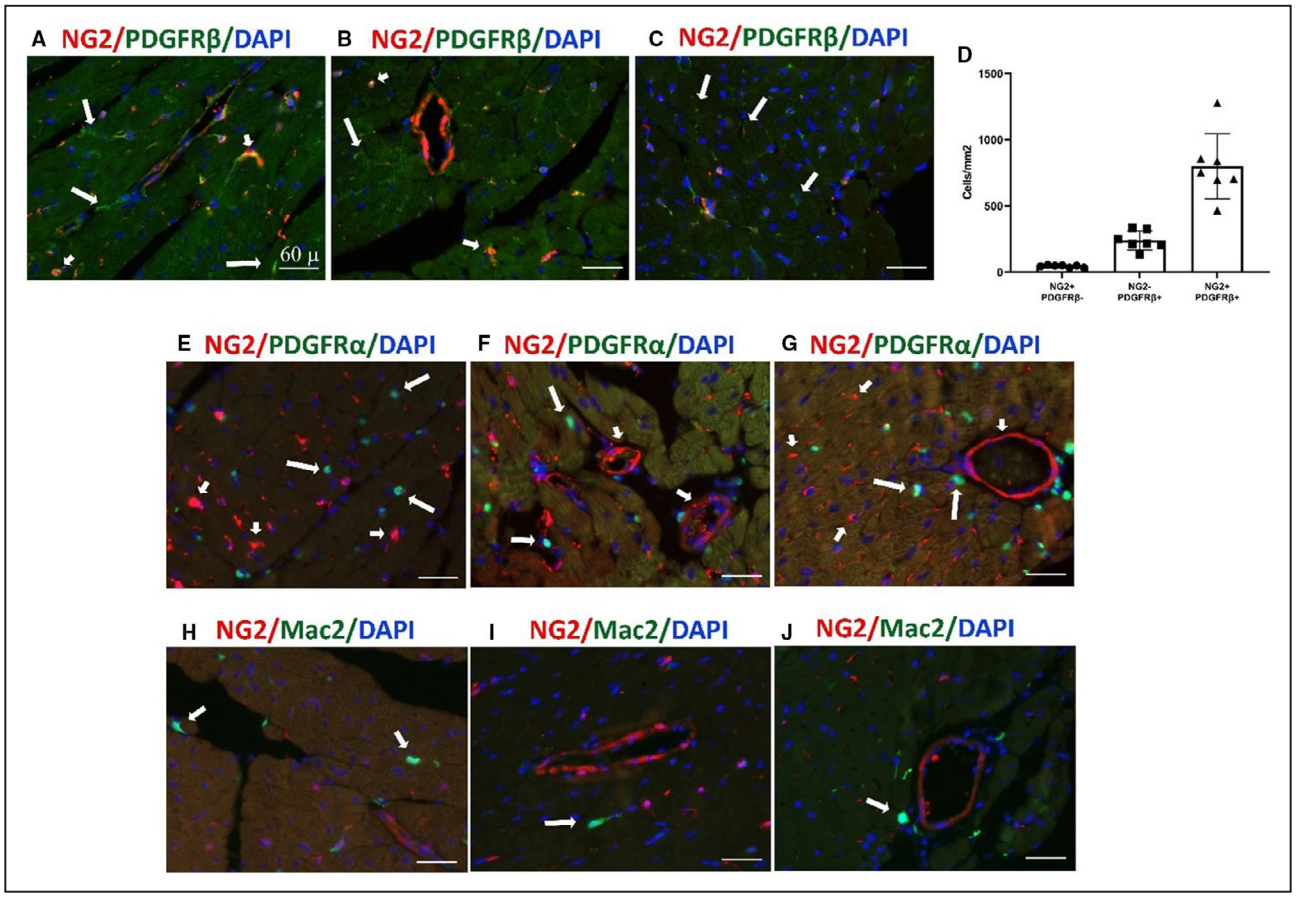

Figure 3. Myocardial neuron-glial antigen 2 (NG2)+ pericytes are platelet-derived growth factor receptor (PDGFR)β+ but do not express the fibroblast marker PDGFRα and the macrophage marker Mac2.
A through **C**, Dual immunofluorescence of $NG2^{Dsred}$ mouse cardiac sections shows that NG2+ pericytes coexpress PDGFRβ (short arrows). A large population of NG2– PDGFRβ+ interstitial cells is also identified (long arrows). **D**, Quantitative analysis (n=7 per group) shows that, although the majority of PDGFRβ+ profiles are also labeled for NG2, there is a large number of PDGFRβ+/NG2– cells. **E** through **G**, To examine potential overlap between NG2+ pericytes and PDGFRα+ fibroblasts, we generated $NG2^{DsRed}$;$PDGFR\alpha^{EGFP}$ dual reporter mice. Dual immunofluorescence shows no overlap of NG2+ pericytes (short arrows) and PDGFRα+ fibroblasts (long arrows). **H** through **J**, Staining of $NG2^{DsRed}$ mouse cardiac sections with the macrophage marker Mac2 was performed to examine whether NG2 labels macrophages. NG2+ pericytes do not express Mac2. A relatively small number of Mac2+ macrophages is noted in the mouse myocardium (arrows). Images are representative of 6 different experiments. Scale bar=60 μm. Data are expressed as mean±SE. Dsred indicates Discosoma species red; and EGFP enhanced green fluorescent protein.

PDGFRα+ and NG2+ cells had distinct transcriptomic profiles (Figure 4B through 4R, Figure S4). PDGFRα+ cells expressed much higher levels of fibrillar collagens (*col1a1, col3a1, col5a1*, and *col6a1*; Figure 4C through 4F), matrix metalloproteinases, tissue inhibitor of metalloproteinases (*Mmp1a, Mmp2, Timp2*, and *Timp3*; Figure 4G through 4J), and genes encoding matricellular proteins (*Sparc, Thbs2, Thbs3*, and *Ccn2*; Figure 4K through 4N). In contrast, NG2+ cells had higher levels of *Adamts1* and *Vtn*. Quantitative PCR also showed that NG2+ cells had much higher levels of expression of the mural cell gene *Pdgfrb* and a trend towards higher expression of *Acta2* (Figure 4O through 4R), Thus, the transcriptomic data suggest that NG2+ cells and PDGFRα+ cells represent 2 distinct cell types with characteristics of myocardial mural cells and fibroblasts, respectively.

Tracing of NG2+ Cells Using a Germline NG2-Cre Driver Labels Cardiomyocytes

We first used a germline NG2-Cre line to label mural cells in mouse hearts. $NG2^{Cre/+}$ animals were bred with $R26^{EYFP}$ mice. $NG2^{Cre/+}$;$R26^{EYFP}$ mice were euthanized at 2 to 3 months of age and the hearts were harvested for histological studies. Dual fluorescence for enhanced yellow fluorescent protein and the endothelial cell marker CD31 showed that vascular mural cells could not be specifically identified. In contrast, there was intense cardiomyocyte labeling with individual variations between cells (Figure S5).

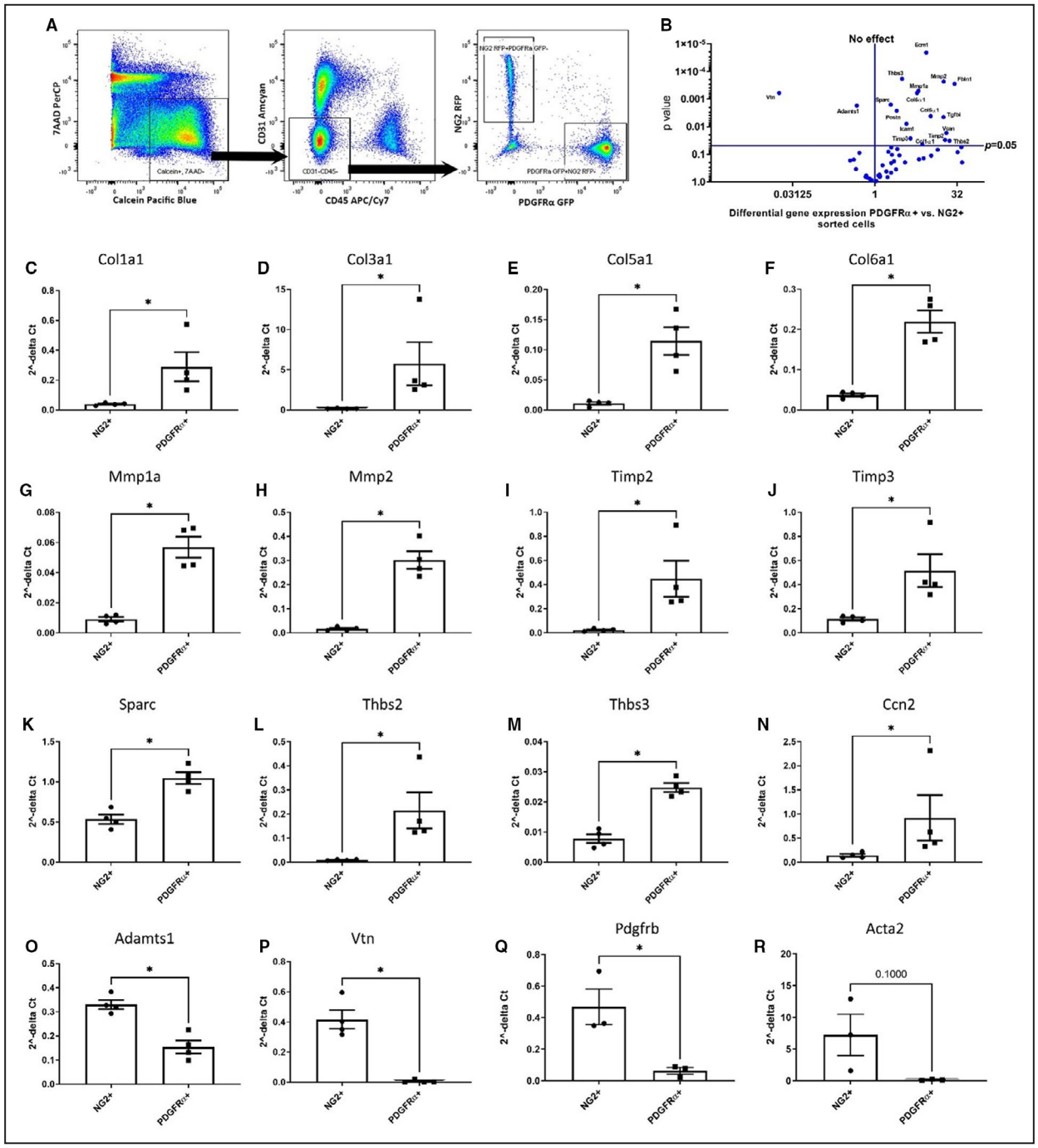

Figure 4. Myocardial neuron-glial antigen 2 (NG2)+ pericytes and platelet-derived growth factor receptor (PDGFR)α+ fibroblasts have distinct transcriptomic profiles.

A, Single-cell suspension was prepared from dual reporter NG2^{DsRed};PDGFRα^{EGFP} hearts using a collagenase/dispase-based enzymatic procedure. Viable (7-aminoactinomycin D/7-AAD) and metabolically active (calcein+) cells were gated and based on the expression of CD31 and CD45, the nonendothelial and nonhematopoietic cell population was identified and subgated. NG2+ and PDGFRα+ populations were sorted by fluorescence-assisted cell sorter into cell lysis buffer to isolate RNA. **B**, The volcano plot summarizes the extracellular matrix array quantitative polymerase chain reaction (PCR) data. **C** through **P**, PDGFRα+ cells have higher levels of matrix-related genes, such as *Col1α1*(**C**), *Col3α1* (**D**), *Col5α1* (**E**), *Col6α1* (**F**), *Mmp1α* (**G**), *Mmp2* (**H**), *Timp2* (**I**), *Timp*3 (**J**), and genes encoding matricellular proteins, including Sparc (**K**), *Thbs2* (**L**), *Thbs3* (**M**), and *Ccn2* (**N**). On the other hand, NG2+ cells expressed higher levels of *Adamts1* (**O**) and *Vtn* (**P**) (**P*=0.05; n=4). **Q** and **R**, Quantitative PCR showed that NG2+ pericytes had higher levels of *Pdgfrb* (**Q**) and a trend toward higher expression of *Acta2* (*P*=0.1; R) (n=3; **P*<0.05). Data are expressed as mean±SE. Statistical comparisons were performed using unpaired *t* test for normal distributions and Mann-Whitney test for non-Gaussian distributions. Dsred indicates Discosoma species red; and EGFP enhanced green fluorescent protein.

Inducible NG2CreER^{TM} Line Specifically Labels Mural Cells in the Myocardium and in the Aorta

Because labeling of cardiomyocytes precluded identification of pericyte-derived cells in the constitutive NG2Cre mice, we tested whether the inducible NG2CreER^{TM} line can be used to trace pericytes in the myocardium. NG2CreER^{TM} mice were crossed with R26^{tdTomato} animals (Figure 5A). NG2$^{iCre/+}$;R26^{tdTomato} mice were injected with tamoxifen at 3 months of age. Heart and ascending aorta were harvested 2 days after the last injection and used for histological analysis. In both atria and ventricles, a large population of periendothelial mural cells was labeled, without staining of cardiomyocytes (Figure 5B). Although there was a trend towards increased density of NG2-traced cells in the ventricles, in comparison to the atria, the differences did not reach statistical significance (Figure 5C). Lineage tracing using the NG2CreER^{TM} line also labeled a significant population of valvular cells, which were more abundant in the aortic valve (Figure S6A and S6B). In the aorta, 60.7%±5.2% of aortic medial α-SMA+VSMCs were labeled with the inducible NG2-Cre driver (Figure S6C through S6H).

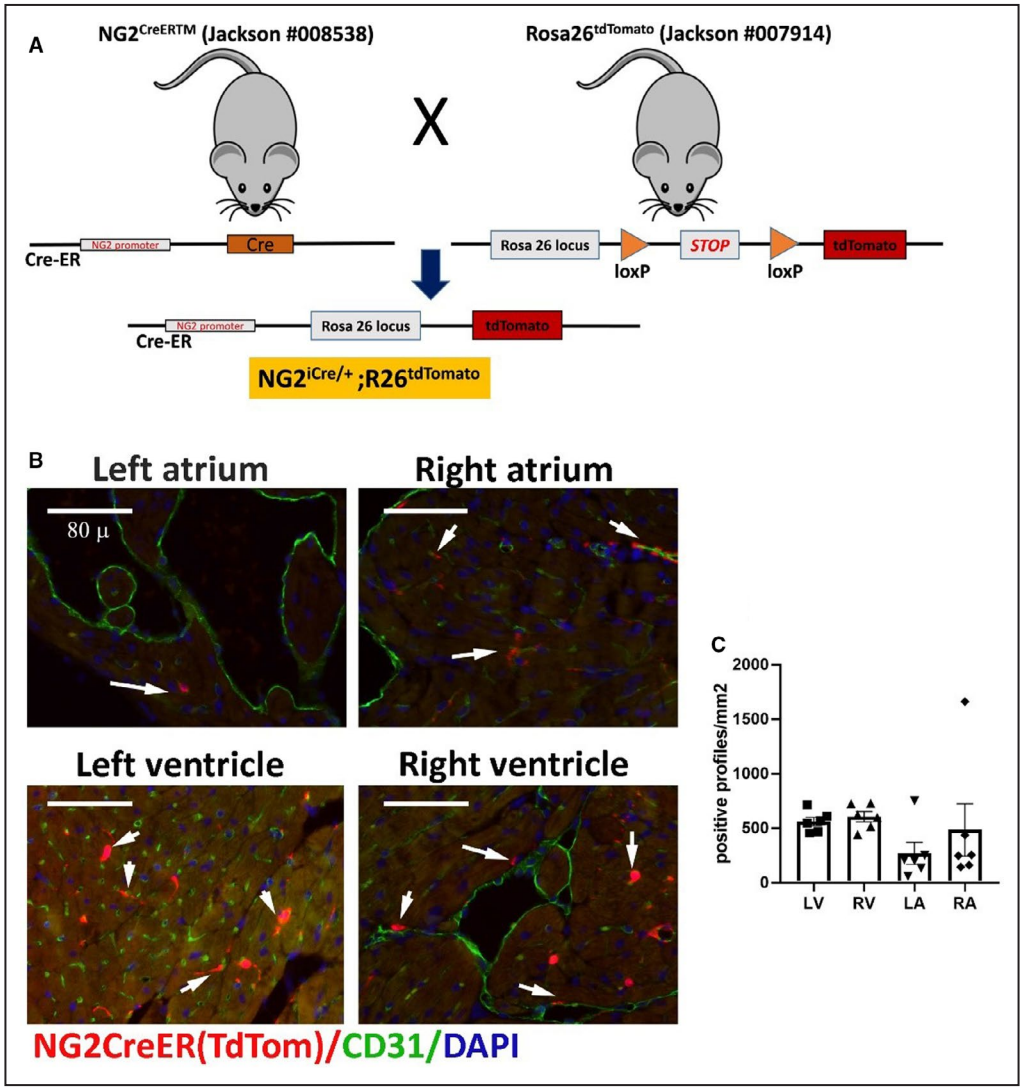

Figure 5. The inducible neuron-glial antigen 2 (NG2) tamoxifen-inducible Cre recombinase (CreER^{TM}) line specifically labels myocardial pericytes.
A, The schematic cartoon shows the breeding scheme used to develop NG2$^{iCre/+}$; Rosa26^{tdTomato} mice. NG2CreER^{TM} mice were crossed with Rosa26^{tdTomato} animals and the resultant NG2$^{iCre/+}$;R26^{tdTomato} mice were injected with tamoxifen at 3 months of age. **B** and **C**, NG2+ pericytes identified using the lineage tracing approach are closely associated with CD31+ endothelial cells. Quantitative analysis (n=6) shows the density of NG2-derived cells in all cardiac chambers (**C**). Scalebar=80 µm. Data are expressed as mean±SE. Statistical comparison was performed using nonparametric ANOVA (Kruskal-Wallis, *P*=not significant). LA indicates left atrium; LV, left ventricle; RA, right atrium; Rosa, reverse orientation splice acceptor; RV, right ventricle; and tdTom, tandem dimer Tomato.

Inducible PDGFRβCreER^{T2} Driver Labels Abundant Myocardial Interstitial Cells, Including Mural Cells and a Significant Fraction of Cardiac Fibroblasts

Next, we used the inducible PDGFRβCreER^{T2} line to trace mural cells in the myocardium and the aorta. PDGFRβCreER^{T2} mice were bred with R26^{tdTomato} animals. PDGFRβ$^{iCre/+}$;R26^{tdTomato} mice (Figure 6A) were injected with tamoxifen and euthanized within a week. The heart and the ascending aorta were used for histological analysis. Dual immunofluorescence for tdTomato and CD31 showed that abundant myocardial interstitial cells were labeled for PDGFRβ, with both periendothelial and interstitial localizations. In comparison to the inducible NG2-Cre driver, the inducible PDGFRβ-Cre line labeled many more myocardial cells, the majority of which had interstitial nonperiendothelial localization (Figure 6B). In contrast to the NG2 reporter, no significant differences between the density of atrial and ventricular cells were noted, reflecting the abundance of atrial interstitial cells labeled with the inducible PDGFRβ-Cre driver (Figure 6C).

In a similar manner, the PDGFRβ-Cre driver labeled several times more valvular cells than the inducible NG2-Cre driver (Figure S7A and S7B). In the ascending aorta, in addition to labeling a large fraction (69.6%±10.87%) of aortic medial VSMCs, the PDGFRβ-Cre driver also stained a large number of adventitial α-SMA– cells (Figure S7C through S7H).

Because of the interstitial nonperiendothelial localization of many myocardial cells labeled with the PDGFRβ-Cre driver, we postulated that this driver may also label cardiac fibroblasts. To test this hypothesis, we crossed the NG2$^{iCre/+}$;R26^{tdTomato} and the PDGFRβ$^{iCre/+}$;R26^{tdTomato} mice with fibroblast reporter PDGFRα^{EGFP} mice (Figure 7A and 7B). Significant populations of perivascular and interstitial cells labeled with the inducible PDGFRβ-Cre driver also expressed PDGFRα and were identified as fibroblasts (Figure 7C and 7D). In contrast, very few NG2-derived cells exhibited PDGFRα staining in the ventricles or atria (Figure 7E). Quantitative analysis showed that the number of PDGFRα+ fibroblasts labeled with the inducible PDGFRβ-Cre driver were much higher than the fibroblasts labeled with the inducible NG2-Cre driver (Figure 7F). Also, 58.2%±3.42% (n=8) of ventricular PDGFRα+ fibroblasts were labeled for PDGFRβ; in contrast, only 2.3%±0.3% (n=6) of fibroblasts were traced with the inducible NG2-Cre driver (Figure 7G). These findings demonstrated that PDGFRβ is a suboptimal marker to trace pericytes, as it also identifies a significant subset of resident cardiac fibroblasts at baseline. In a similar manner, in the ascending aorta, many of the adventitial cells traced with the inducible PDGFRβ-Cre driver were identified as fibroblasts, on the basis of PDGFRα staining (Figure 8A through 8C). Quantitative analysis showed that 56.4%±6.8% of PDGFRα+ adventitial fibroblasts were also labeled for PDGFRβ (Figure 8D) In contrast, the inducible NG2-driver did not label any adventitial fibroblasts (Figure 8E). Taken together, the findings demonstrate that the inducible PDGFRβ-Cre driver is not specific for mural cells, but also tracks the majority of cardiac and aortic adventitial fibroblasts.

DISCUSSION

We report the first systematic characterization of genetic tools for identification, labeling, and tracing of mouse cardiac pericytes. Using NG2^{DsRed};PDGFRα^{EGFP} dual reporter mice, we identified morphologically and transcriptomically distinct myocardial populations of fibroblasts (PDGFRα+/NG2–) and mural cells (NG2+/PDGFRα–). To evaluate the specificity of pericyte Cre drivers, we crossed 3 different mouse lines that have been extensively used to trace and target pericytes with the well-documented and specific PDGFRα^{EGFP} fibroblast reporter.[37,38] We found that only the inducible NG2-CreER line is specific for mural cells. In contrast, the germline NG2-Cre line is of limited value, as it also labels cardiomyocytes, whereas use of the inducible PDGFRβCreER^{T2} results in Cre-mediated recombination not only in mural cells, but also in the majority of cardiac fibroblasts. Our findings establish optimal strategies for identification and targeting of cardiac pericytes in mice.

Cardiac Pericytes: Abundant Yet Enigmatic

Early ultrastructural studies have identified a large population of pericytes in mammalian hearts. Myocardial

Figure 6. The inducible platelet-derived growth factor receptor (PDGFR)βCreER^{T2} driver labels not only periendothelial cells but also a large population of myocardial interstitial cells, which are not associated with vessels.
A, Breeding strategy shows the development of PDGFRβ$^{iCre/+}$;R26^{tdTomato} model. **B**, Abundant PDGFRβ+ cells are identified in all cardiac chambers using the lineage tracing approach. Please note that the density of the PDGFRβ+ cells is much higher than the numbers of neuron-glial antigen 2 (NG2)+ cells (shown in Figure 5). Dual fluorescence with CD31 shows that a significant proportion of these cells is not associated with endothelial cells. **C**, Quantitative analysis (n=8) of the density of PDGFRβ+ cells in atria and ventricles. Scalebar=100 μm. Data are expressed as mean±SE. Statistical comparison was performed using nonparametric ANOVA (Kruskal-Wallis, *P*=not significant). LA indicates left atrium; LV, left ventricle; RA, right atrium; RV, right ventricle; and tdTom, tandem dimer Tomato.

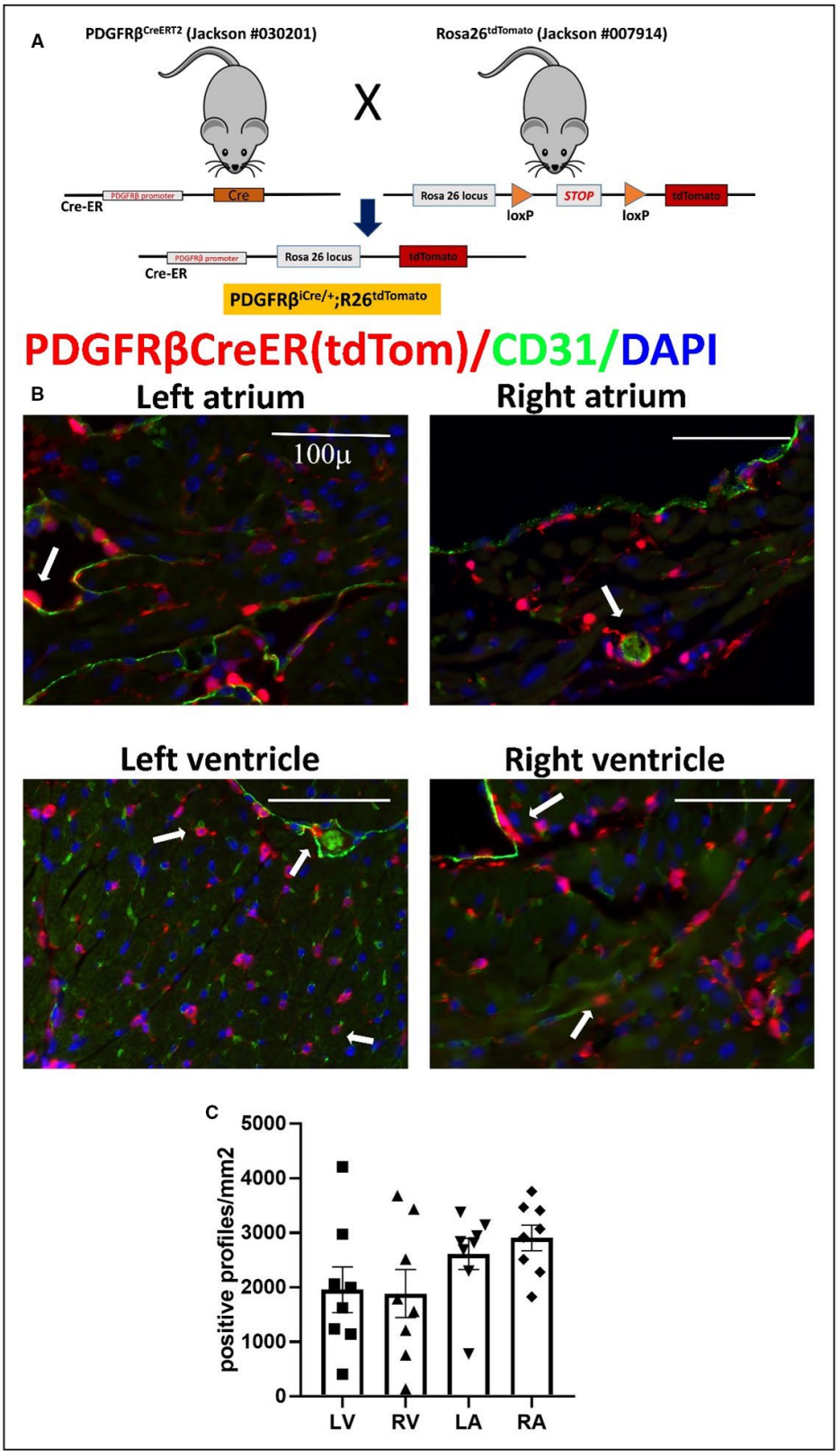

pericytes were described as extensively branched cells that form an incomplete layer around the endothelium[39] and express contractile proteins,[40] findings consistent with their proposed role in regulation of microvascular blood flow. Data on the relative abundance of pericytes in mammalian hearts are conflicting and are

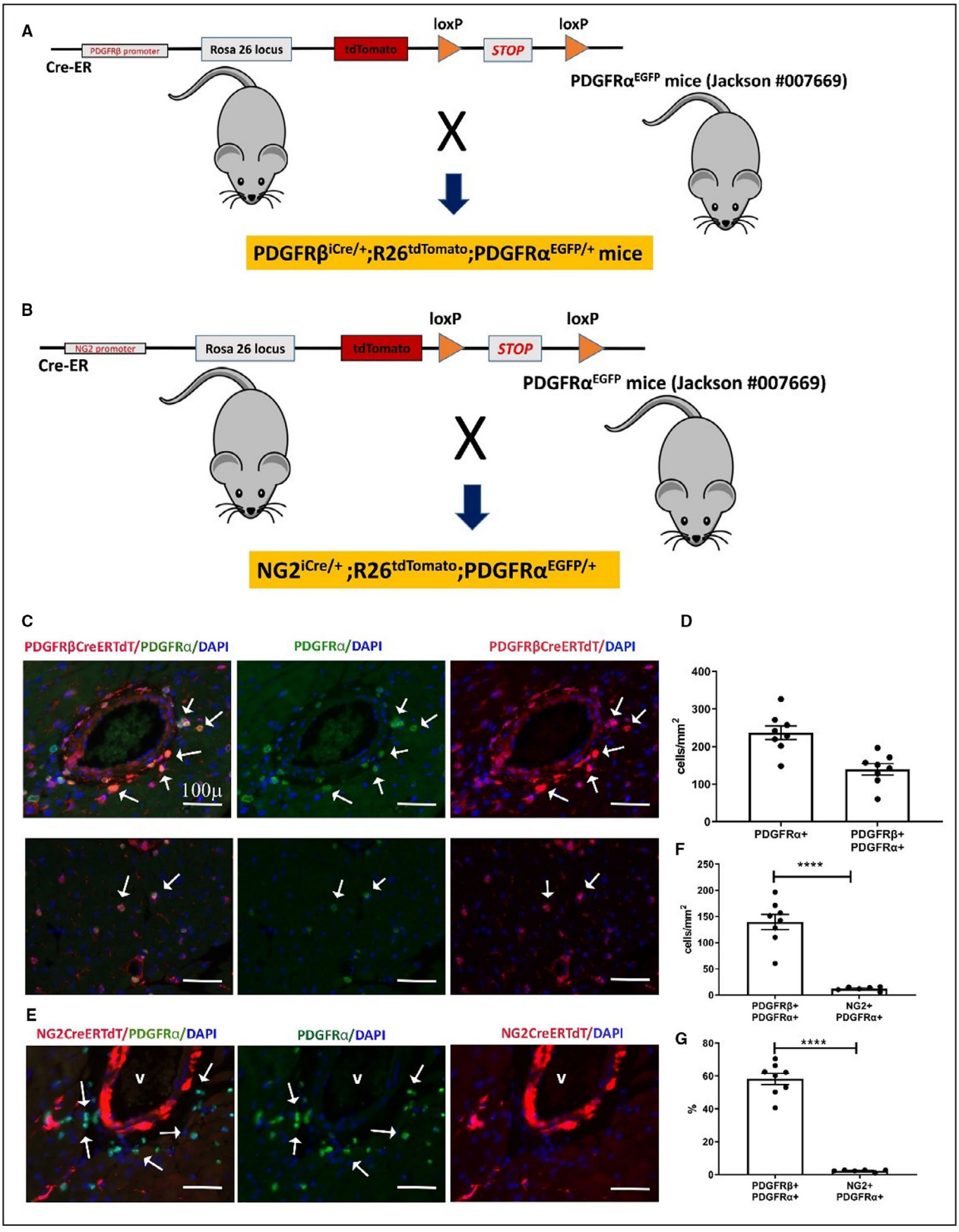

dependent on the species studied, and on the methodology used for their identification. A highly systematic study that isolated myocardial pericytes from several different species reported that pericytes may be more abundant than cardiomyocytes, thus representing the second most frequent myocardial cell type in the rat heart, outnumbered only by endothelial cells.[24] In contrast, other investigations using single markers for flow

Figure 7. The neuron-glial antigen 2 (NG2) tamoxifen-inducible Cre recombinase (CreER^{TM}) driver specifically labels mural cells, whereas the inducible platelet-derived growth factor receptor (PDGFR)βCreER^{T2} line lacks specificity, also labeling a significant fraction of PDGFRα+ cardiac fibroblasts.

A and **B**, To test the specificity of the inducible PDGFRβ and NG2-Cre drivers for myocardial pericytes, we bred PDGRβ$^{iCre/+}$;R26^{tdTomato} mice (**A**), and NG2$^{iCre/+}$;R26^{tdTomato} animals (**B**) with fibroblast reporter PDGFRα^{EGFP} mice. Schematic cartoons show the breeding scheme. **C**, Dual immunofluorescence of left ventricular sections shows that the inducible PDGFRβ-Cre driver lacks specificity, labeling a large fraction of perivascular fibroblasts (**C**, top row) and interstitial fibroblasts (**C**, lower row) in the myocardium. PDGFRβ+/PDGFRα+ fibroblasts are indicated with arrows. **D**, Quantitative analysis (n=8) shows the density of PDGFRα+ fibroblasts and PDGFRα+/PDGFRβ+ fibroblasts in the myocardium. **E**, In NG2$^{iCre/+}$;R26^{tdTomato};PDGFRα^{EGFP} mice, staining for tandem dimer Tomato (tdTom) and green fluorescent protein shows that cardiac fibroblasts are not labeled for NG2, supporting the specificity of the inducible NG2-Cre line. **F**, Quantitative analysis shows that the number of PDGFRβ+ cells identified as fibroblasts is markedly higher than the number of NG2+ cells that exhibit PDGFRα expression (****P<0.0001; n=6–8). **G**, Approximately 60% of PDGFRα+ fibroblasts are also labeled for PDGFRβ, whereas the percentage of fibroblasts labeled for NG2 is low (****P<0.0001; n=6–8). Scalebar=100 μm. Data are expressed as mean±SE. Statistical comparisons were performed using unpaired *t* test. DAPI indicates 4',6'-diamidino-2-phenylindole; and EGFP, enhanced green fluorescent protein.

cytometric cell identification suggested that in adult mouse hearts, pericytes are vastly outnumbered by fibroblasts.[19] Data from human hearts are scarce. An ultrastructural study suggested that mural cells (both pericytes and VSMCs) in the left ventricle may be more abundant than fibroblasts, representing ≈22% to 28% of interstitial cells.[41] A recent single-cell transcriptomic study of myocardial samples harvested from deceased organ donors also suggested an abundant population of myocardial pericytes and smooth muscle cells, identifying ≈21% of ventricular cells and ≈17% of atrial cells as mural cells.[20]

Pericytes and Fibroblasts

It should be emphasized that a large fraction of the fibroblast-like interstitial cells in the myocardium exhibit a perivascular location.[42] These cells may share certain common characteristics with pericytes; in fact, in some studies, pericytes have been referred to as "fibroblast-like cells."[43] The most rigorous and accepted definition of a mature pericyte requires demonstration of the localization of the cell within the microvascular basement membrane, a feature that can only be assessed using electron microscopy. Single-cell omics have revealed the remarkable heterogeneity of myocardial interstitial populations in health and disease.[44–46] Despite the unquestionable value of high-resolution definition of the diversity of interstitial cell populations at the single-cell level, identification and classification of cells into traditionally defined types remain critical for understanding the cell biology of myocardial disease. In the current study, we demonstrate that use of the NG2^{DsRed};PDGFRα^{EGFP} dual reporter mouse line allows identification of mural cells and fibroblasts in the mouse heart. No significant overlap between the 2 populations was noted (Figure 3, Figure 4A). Moreover, PDGFRα+/NG2– cells exhibited a transcriptomic profile typical of matrix-synthetic fibroblasts, expressing high levels of fibrillar collagens, matrix metalloproteinases, tissue inhibitor of metalloproteinases, and matricellular genes (Figure 4C through 4N). In contrast, NG2+/PDGFRα– cells expressed low levels of matrix genes but exhibited much higher levels of *Adamts1*, *Vtn*, and *Pdgfrb* expression (Figure 4O through 4Q). High levels of vitronectin expression were previously reported in brain pericytes.[47] In contrast, Adamts1 has not been previously found to be expressed in normal kidney pericytes but has been reported to be highly upregulated upon injury.[48]

Contractile Filament Proteins Lack Specificity for Pericyte Identification

Several "pericyte-specific" markers have been used in attempts to identify pericytes and distinguish them from other interstitial cell types.[49,50] Some of these markers are clearly unreliable, lacking specificity and sensitivity. CD146, also known as melanoma cell adhesion molecule, has been used to identify pericytes[51] but is also highly expressed in endothelial cells.[52–54] On the other hand, vimentin, α-SMA, and desmin are expressed in contractile filaments and have been used to label pericytes in some studies. Vimentin is highly expressed in all mesenchymally derived cells, including fibroblasts and all mural cells.[55] Desmin expression has been variably reported in subsets of fibroblasts and pericytes in several different tissues but is not expressed by myocardial pericytes.[51] α-SMA also has low specificity and sensitivity as a pericyte marker. In comparison to VSMCs, pericytes have low levels of α-SMA expression[56] but upregulate α-SMA synthesis in response to stimulation with growth factors, such as transforming growth factor β.[57] However, the specificity of α-SMA as a marker for activated pericytes is limited by its marked induction in injury-site myofibroblasts.[58,59]

NG2 and PDGFRβ as Pericyte Markers

The proteoglycan NG2 and the growth factor receptor PDGFRβ are the most commonly used markers for pericytes in mouse studies.[50] Anti-NG2 antibodies, NG2^{DsRed} fluorescent reporter mice, and constitutive and inducible NG2-Cre drivers have been extensively used to identify,

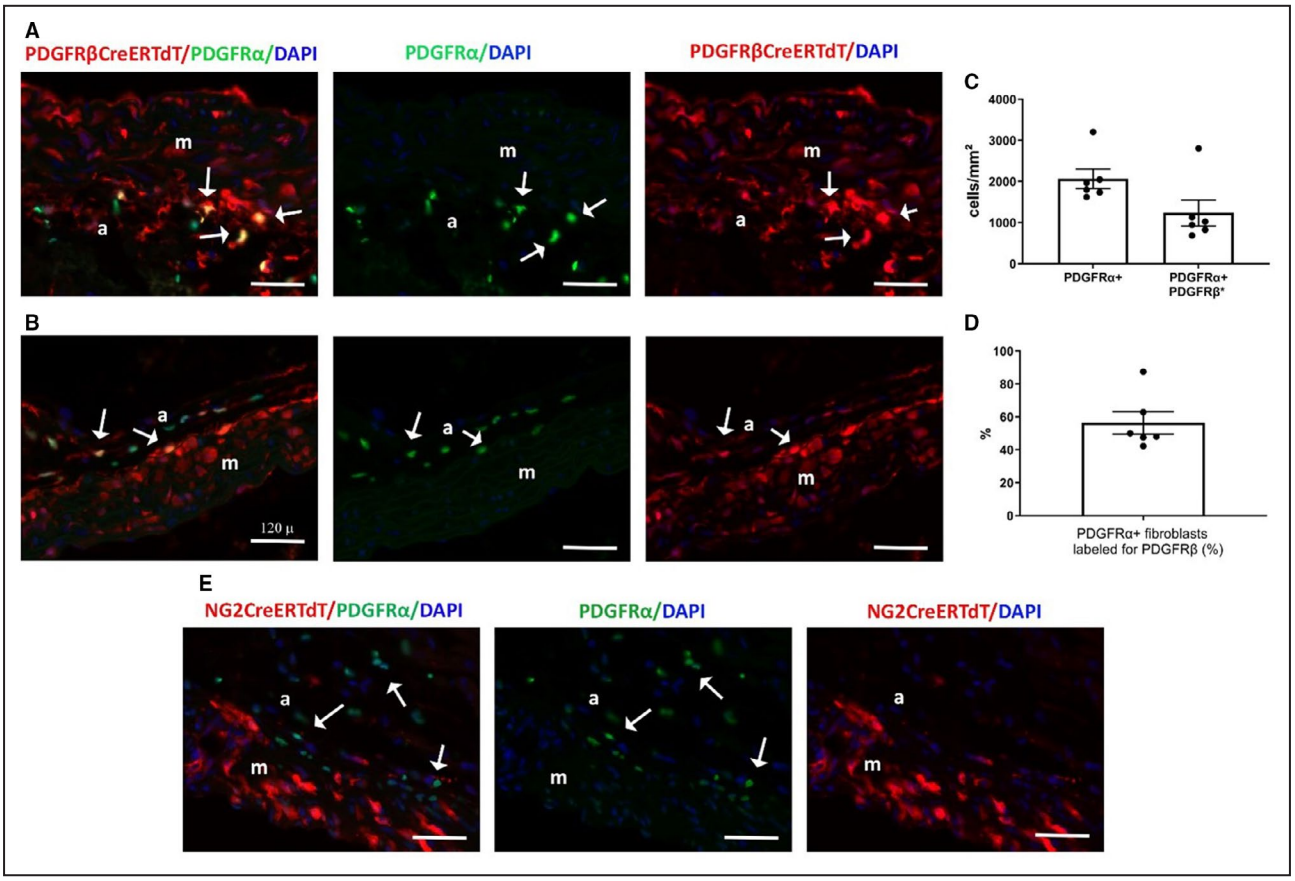

Figure 8. In the ascending aorta, the neuron-glial antigen 2 (NG2) tamoxifen-inducible Cre recombinase (CreER^{TM}) driver is specific for mural cells, whereas the inducible platelet-derived growth factor receptor (PDGFR)βCreER^{T2} driver lacks specificity, also labeling PDGFRα+ aortic adventital fibroblasts.

A through **D**, To test the specificity of the inducible PDGFRβ-Cre driver for aortic mural cells, we bred PDGRβ$^{iCre/+}$;R26^{tdTomato} mice with fibroblast reporter PDGFRα^{EGFP} mice. Dual immunofluorescence of aortic sections shows that the inducible PDGFRβ-Cre driver lacks specificity, labeling a large fraction of PDGFRα+ adventitial fibroblasts (**A**, **C**: arrows). Quantitative analysis shows (n=6) the density of adventitial PDGFRα+ fibroblasts and the density of fibroblasts labeled for PDGFRβ in the ascending aorta (**C**). **D**, More than 50% of adventitial fibroblasts (PDGFRα+ cells) were labeled for PDGFRβ (n=6). **E**, To test the specificity of the inducible NG2-Cre driver, NG2$^{iCre/+}$;R26^{tdTomato} were bred into the PDGFRα^{EGFP} reporter mouse line. Sections from the ascending aorta were stained for tandem dimer Tomato (tdTomato) and green fluorescent protein. Dual fluorescence shows that aortic adventitial fibroblasts (arrows) are not labeled for NG2, supporting the specificity of the inducible NG2-Cre line. Images are representative of 6 different experiments. Scalebar=120 µm. Data are expressed as mean±SE. a indicates adventitia; DAPI, 4',6'-diamidino-2-phenylindole; EGFP, enhanced green fluorescent protein; and m, media.

trace, and target pericytes in vivo.[60–63] PDGFRβ staining has also been used to specifically label pericytes in mouse tissues,[31] and inducible PDGFRβ-Cre drivers have been considered in some studies optimal genetic tools for pericyte-specific targeting.[32,33] However, the frequent use of the same inducible PDGFRβ-Cre drivers to target fibroblast-like interstitial cells[34,35] in other studies generates confusion regarding the specificity of these tools. To evaluate the specificity of NG2 and PDGFRβ-Cre drivers, we crossed these lines with fibroblast-specific PDGFRα reporter mice. Our findings demonstrate that only the inducible NG2-CReER^{TM} line induces recombination specifically in mural cells (Figure 5), showing no significant overlap with myocardial interstitial PDGFRα+ fibroblasts (Figure 7E through 7G). In contrast, the inducible PDGFRβ-Cre driver labeled, in addition to mural cells, ≈60% of PDGFRα+ myocardial perivascular and interstitial fibroblasts (Figure 7G). Similar observations were noted in the aorta. The inducible PDGFRβ-Cre driver targeted not only mural cells in the media and the adventitia but also a large fraction of aortic adventitial fibroblasts (Figure 8A through 8D). In contrast, the inducible NG2-Cre driver specifically labeled mural cells (Figure 8E).

Is There an Optimal Tool for Labeling and Targeting Cardiac Pericytes in Mice?

Single-cell transcriptomic studies indicate that no single transcript qualifies as a specific pan-pericyte

marker.[64] The differences in pericyte populations residing in various tissues and the distinct patterns of diversity of fibroblasts and other interstitial cell types in different organs suggest the need for organ-specific approaches for tracing and targeting pericytes. Our study shows that myocardial mural cells are optimally labeled and targeted by using an inducible NG2-Cre driver. In contrast, the inducible PDGFRβ-Cre driver lacks specificity and may be useful only for manipulation of a broader population of interstitial cells, including a large fraction of fibroblasts.

CONCLUSIONS

Unfortunately, the field of myocardial biology has neglected the pericyte, a cell type of high potential significance in cardiac homeostasis and disease. Associative evidence suggests that pericytes may be involved in early myocardial ischemic injury,[26] may respond to myocardial mechanical stress[25] and neurohumoral stimulation,[9] and may be implicated in fibrosis of the remodeling heart.[65,66] Moreover, some studies have suggested that subpopulations of pericytes may have reparative, angiogenic, and even regenerative potential in models of myocardial injury.[67,68] Thus, experimental studies investigating the role of pericytes in mouse models of heart disease, using well-characterized and validated tools, are critical for understanding cardiac pathophysiology.

ARTICLE INFORMATION

Received July 8, 2021; accepted November 8, 2021.

Affiliation

Department of Medicine (Cardiology), The Wilf Family Cardiovascular Research Institute, Albert Einstein College of Medicine, Bronx, NY.

Sources of Funding

Dr Frangogiannis' laboratory is supported by National Institutes of Health grants R01 HL76246, R01 HL85440, and R01 HL149407 and by U.S. Department of Defense grants PR151029 and PR181464. Dr Tuleta is supported by a postdoctoral grant from the Deutsche Forschungsgemeinschaft (TU 632/1-1).

Disclosures

None.

Supplementary Material

Figures S1–S7

REFERENCES

1. Gaengel K, Genove G, Armulik A, Betsholtz C. Endothelial-mural cell signaling in vascular development and angiogenesis. *Arterioscler Thromb Vasc Biol*. 2009;29:630–638. doi: 10.1161/ATVBAHA.107.161521
2. Sweeney M, Foldes G. It takes two: endothelial-perivascular cell cross-talk in vascular development and disease. *Front Cardiovasc Med*. 2018;5:154. doi: 10.3389/fcvm.2018.00154
3. Armulik A, Genove G, Betsholtz C. Pericytes: developmental, physiological, and pathological perspectives, problems, and promises. *Dev Cell*. 2011;21:193–215. doi: 10.1016/j.devcel.2011.07.001
4. Dulmovits BM, Herman IM. Microvascular remodeling and wound healing: a role for pericytes. *Int J Biochem Cell Biol*. 2012;44:1800–1812. doi: 10.1016/j.biocel.2012.06.031
5. Hall CN, Reynell C, Gesslein B, Hamilton NB, Mishra A, Sutherland BA, O'Farrell FM, Buchan AM, Lauritzen M, Attwell D. Capillary pericytes regulate cerebral blood flow in health and disease. *Nature*. 2014;508:55–60. doi: 10.1038/nature13165
6. Pallone TL, Silldorff EP. Pericyte regulation of renal medullary blood flow. *Exp Nephrol*. 2001;9:165–170. doi: 10.1159/000052608
7. Hartmann DA, Berthiaume AA, Grant RI, Harrill SA, Koski T, Tieu T, McDowell KP, Faino AV, Kelly AL, Shih AY. Brain capillary pericytes exert a substantial but slow influence on blood flow. *Nat Neurosci*. 2021;24:633–645. doi: 10.1038/s41593-020-00793-2
8. Gonzales AL, Klug NR, Moshkforoush A, Lee JC, Lee FK, Shui B, Tsoukias NM, Kotlikoff MI, Hill-Eubanks D, Nelson MT. Contractile pericytes determine the direction of blood flow at capillary junctions. *Proc Natl Acad Sci USA*. 2020;117:27022–27033. doi: 10.1073/pnas.1922755117
9. Špiranec Spes K, Chen W, Krebes L, Völker K, Abeßer M, Eder Negrin P, Cellini A, Nickel A, Nikolaev VO, Hofmann F, et al. Heart-microcirculation connection: effects of ANP (Atrial Natriuretic Peptide) on pericytes participate in the acute and chronic regulation of arterial blood pressure. *Hypertension*. 2020;76:1637–1648. doi: 10.1161/HYPERTENSIONAHA.120.15772
10. Armulik A, Genové G, Mäe M, Nisancioglu MH, Wallgard E, Niaudet C, He L, Norlin J, Lindblom P, Strittmatter K, et al. Pericytes regulate the blood-brain barrier. *Nature*. 2010;468:557–561. doi: 10.1038/nature09522
11. Daneman R, Zhou L, Kebede AA, Barres BA. Pericytes are required for blood-brain barrier integrity during embryogenesis. *Nature*. 2010;468:562–566. doi: 10.1038/nature09513
12. Török O, Schreiner B, Schaffenrath J, Tsai HC, Maheshwari U, Stifter SA, Welsh C, Amorim A, Sridhar S, Utz SG, et al. Pericytes regulate vascular immune homeostasis in the CNS. *Proc Natl Acad Sci USA*. 2021;118:e2016587118. doi: 10.1073/pnas.2016587118
13. Pellowe AS, Sauler M, Hou Y, Merola J, Liu R, Calderon B, Lauridsen HM, Harris MR, Leng L, Zhang YI, et al. Endothelial cell-secreted MIF reduces pericyte contractility and enhances neutrophil extravasation. *FASEB J*. 2019;33:2171–2186. doi: 10.1096/fj.201800480R
14. Shaw I, Rider S, Mullins J, Hughes J, Peault B. Pericytes in the renal vasculature: roles in health and disease. *Nat Rev Nephrol*. 2018;14:521–534. doi: 10.1038/s41581-018-0032-4
15. Greenhalgh SN, Iredale JP, Henderson NC. Origins of fibrosis: pericytes take centre stage. *F1000prime Reports*. 2013;5:37. doi: 10.12703/P5-37
16. Kramann R, Humphreys BD. Kidney pericytes: roles in regeneration and fibrosis. *Semin Nephrol*. 2014;34:374–383. doi: 10.1016/j.semnephrol.2014.06.004
17. Garza Trevino EN, Gonzalez PD, Valencia Salgado CI, Martinez GA. Effects of pericytes and colon cancer stem cells in the tumor microenvironment. *Cancer Cell Int*. 2019;19:173. doi: 10.1186/s12935-019-0888-9
18. Paiva AE, Lousado L, Guerra DA, Azevedo PO, Sena IF, Andreotti JP, Santos GS, Goncalves R, Mintz A, Birbrair A. Pericytes in the premetastatic niche. *Cancer Res*. 2018;78:2779–2786. doi: 10.1158/0008-5472.CAN-17-3883
19. Pinto AR, Ilinykh A, Ivey MJ, Kuwabara JT, D'Antoni ML, Debuque R, Chandran A, Wang L, Arora K, Rosenthal NA, et al. Revisiting cardiac cellular composition. *Circ Res*. 2016;118:400–409. doi: 10.1161/CIRCRESAHA.115.307778
20. Litviňuková M, Talavera-López C, Maatz H, Reichart D, Worth CL, Lindberg EL, Kanda M, Polanski K, Heinig M, Lee M, et al. Cells of the adult human heart. *Nature*. 2020;588:466–472. doi: 10.1038/s41586-020-2797-4
21. Lee LL, Khakoo AY, Chintalgattu V. Cardiac pericytes function as key vasoactive cells to regulate homeostasis and disease. *FEBS Open Bio*. 2021;11:207–225. doi: 10.1002/2211-5463.13021
22. Avolio E, Madeddu P. Discovering cardiac pericyte biology: from physiopathological mechanisms to potential therapeutic applications in ischemic heart disease. *Vascul Pharmacol*. 2016;86:53–63. doi: 10.1016/j.vph.2016.05.009
23. Alex L, Frangogiannis NG. Pericytes in the infarcted heart. *Vasc Biol*. 2019;1:H23–H31. doi: 10.1530/VB-19-0007
24. Nees S, Weiss DR, Senftl A, Knott M, Forch S, Schnurr M, Weyrich P, Juchem G. Isolation, bulk cultivation, and characterization of coronary microvascular pericytes: the second most frequent myocardial cell

type in vitro. *Am J Physiol Heart Circ Physiol*. 2012;302:H69–H84. doi: 10.1152/ajpheart.00359.2011
25. Rolle IG, Crivellari I, Zanello A, Mazzega E, Dalla E, Bulfoni M, Avolio E, Battistella A, Lazzarino M, Cellot A, et al. Heart failure impairs the mechanotransduction properties of human cardiac pericytes. *J Mol Cell Cardiol*. 2021;151:15–30. doi: 10.1016/j.yjmcc.2020.10.016
26. Siao CJ, Lorentz CU, Kermani P, Marinic T, Carter J, McGrath K, Padow VA, Mark W, Falcone DJ, Cohen-Gould L, et al. ProNGF, a cytokine induced after myocardial infarction in humans, targets pericytes to promote microvascular damage and activation. *J Exp Med*. 2012;209:2291–2305. doi: 10.1084/jem.20111749
27. O'Farrell FM, Attwell D. A role for pericytes in coronary no-reflow. *Nat Rev Cardiol*. 2014;11:427–432. doi: 10.1038/nrcardio.2014.58
28. O'Farrell FM, Mastitskaya S, Hammond-Haley M, Freitas F, Wah WR, Attwell D. Capillary pericytes mediate coronary no-reflow after myocardial ischaemia. *Elife*. 2017;6. doi: 10.7554/eLife.29280
29. Chintalgattu V, Rees ML, Culver JC, Goel A, Jiffar T, Zhang J, Dunner K, Pati S, Bankson JA, Pasqualini R, et al. Coronary microvascular pericytes are the cellular target of sunitinib malate-induced cardiotoxicity. *Sci Transl Med*. 2013;5:187ra169. doi: 10.1126/scitranslmed.3005066
30. Tallquist MD. Cardiac fibroblast diversity. *Annu Rev Physiol*. 2020;82:63–78. doi: 10.1146/annurev-physiol-021119-034527
31. Winkler EA, Bell RD, Zlokovic BV. Pericyte-specific expression of PDGF beta receptor in mouse models with normal and deficient PDGF beta receptor signaling. *Mol Neurodegener*. 2010;5:32. doi: 10.1186/1750-1326-5-32
32. Cuervo H, Pereira B, Nadeem T, Lin M, Lee F, Kitajewski J, Lin CS. PDGFRbeta-P2A-CreER(T2) mice: a genetic tool to target pericytes in angiogenesis. *Angiogenesis*. 2017;20:655–662. doi: 10.1007/s10456-017-9570-9
33. Špiranec K, Chen W, Werner F, Nikolaev VO, Naruke T, Koch F, Werner A, Eder-Negrin P, Diéguez-Hurtado R, Adams RH, et al. Endothelial C-type natriuretic peptide acts on pericytes to regulate microcirculatory flow and blood pressure. *Circulation*. 2018;138:494–508. doi: 10.1161/CIRCULATIONAHA.117.033383
34. Henderson NC, Arnold TD, Katamura Y, Giacomini MM, Rodriguez JD, McCarty JH, Pellicoro A, Raschperger E, Betsholtz C, Ruminski PG, et al. Targeting of αv integrin identifies a core molecular pathway that regulates fibrosis in several organs. *Nat Med*. 2013;19:1617–1624. doi: 10.1038/nm.3282
35. Sciurba JC, Gieseck RL, Jiwrajka N, White SD, Karmele EP, Redes J, Vannella KM, Henderson NC, Wynn TA, Hart KM. Fibroblast-specific integrin-alpha V differentially regulates type 17 and type 2 driven inflammation and fibrosis. *J Pathol*. 2019;248:16–29. doi: 10.1002/path.5215
36. Stallcup WB. The NG2 proteoglycan in pericyte biology. *Adv Exp Med Biol*. 2018;1109:5–19. doi: 10.1007/978-3-030-02601-1_2
37. Ivey MJ, Kuwabara JT, Riggsbee KL, Tallquist MD. Platelet derived growth factor receptor alpha is essential for cardiac fibroblast survival. *Am J Physiol Heart Circ Physiol*. 2019;317:H330–H344. doi: 10.1152/ajpheart.00054.2019
38. Smith CL, Baek ST, Sung CY, Tallquist MD. Epicardial-derived cell epithelial-to-mesenchymal transition and fate specification require PDGF receptor signaling. *Circ Res*. 2011;108:e15–e26. doi: 10.1161/CIRCRESAHA.110.235531
39. Forbes MS, Rennels ML, Nelson E. Ultrastructure of pericytes in mouse heart. *Am J Anat*. 1977;149:47–70. doi: 10.1002/aja.1001490105
40. Joyce NC, Haire MF, Palade GE. Contractile proteins in pericytes. I. Immunoperoxidase localization of tropomyosin. *J Cell Biol*. 1985;100:1379–1386. doi: 10.1083/jcb.100.5.1379
41. Popescu LM, Curici A, Wang E, Zhang H, Hu S, Gherghiceanu M. Telocytes and putative stem cells in ageing human heart. *J Cell Mol Med*. 2015;19:31–45. doi: 10.1111/jcmm.12509
42. Di Carlo SE, Peduto L. The perivascular origin of pathological fibroblasts. *J Clin Invest*. 2018;128:54–63. doi: 10.1172/JCI93558
43. Hsia LT, Ashley N, Ouaret D, Wang LM, Wilding J, Bodmer WF. Myofibroblasts are distinguished from activated skin fibroblasts by the expression of AOC3 and other associated markers. *Proc Natl Acad Sci USA*. 2016;113:E2162–E2171. doi: 10.1073/pnas.1603534113
44. Farbehi N, Patrick R, Dorison A, Xaymardan M, Janbandhu V, Wystub-Lis K, Ho JW, Nordon RE, Harvey RP. Single-cell expression profiling reveals dynamic flux of cardiac stromal, vascular and immune cells in health and injury. *Elife*. 2019;8:e43882. doi: 10.7554/eLife.43882
45. McLellan MA, Skelly DA, Dona MSI, Squiers GT, Farrugia GE, Gaynor TL, Cohen CD, Pandey R, Diep H, Vinh A, et al. High-resolution transcriptomic profiling of the heart during chronic stress reveals cellular drivers of cardiac fibrosis and hypertrophy. *Circulation*. 2020;142:1448–1463. doi: 10.1161/CIRCULATIONAHA.119.045115
46. Wang LI, Yang Y, Ma H, Xie Y, Xu J, Near D, Wang H, Garbutt T, Li Y, Liu J, et al. Single cell dual-omics reveals the transcriptomic and epigenomic diversity of cardiac non-myocytes. *Cardiovasc Res*. 2021. doi: 10.1093/cvr/cvab134
47. He L, Vanlandewijck M, Raschperger E, Andaloussi Mae M, Jung B, Lebouvier T, Ando K, Hofmann J, Keller A, Betsholtz C. Analysis of the brain mural cell transcriptome. *Sci Rep*. 2016;6:35108. doi: 10.1038/srep35108
48. Schrimpf C, Xin C, Campanholle G, Gill SE, Stallcup W, Lin SL, Davis GE, Gharib SA, Humphreys BD, Duffield JS. Pericyte TIMP3 and ADAMTS1 modulate vascular stability after kidney injury. *J Am Soc Nephrol*. 2012;23:868–883. doi: 10.1681/ASN.2011080851
49. Yamazaki T, Mukouyama YS. Tissue specific origin, development, and pathological perspectives of pericytes. *Front Cardiovasc Med*. 2018;5:78. doi: 10.3389/fcvm.2018.00078
50. Hartmann DA, Underly RG, Watson AN, Shih AY. A murine toolbox for imaging the neurovascular unit. *Microcirculation*. 2015;22:168–182. doi: 10.1111/micc.12176
51. Chen WC, Baily JE, Corselli M, Diaz ME, Sun B, Xiang G, Gray GA, Huard J, Peault B. Human myocardial pericytes: multipotent mesodermal precursors exhibiting cardiac specificity. *Stem Cells*. 2015;33:557–573. doi: 10.1002/stem.1868
52. Wang Z, Xu Q, Zhang N, Du X, Xu G, Yan X. CD146, from a melanoma cell adhesion molecule to a signaling receptor. *Signal Transduct Target Ther*. 2020;5:148. doi: 10.1038/s41392-020-00259-8
53. Ren G, Michael LH, Entman ML, Frangogiannis NG. Morphological characteristics of the microvasculature in healing myocardial infarcts. *J Histochem Cytochem*. 2002;50:71–79. doi: 10.1177/002215540205000108
54. Anfosso F, Bardin N, Francès V, Vivier E, Camoin-Jau L, Sampol J, Dignat-George F. Activation of human endothelial cells via S-Endo-1 antigen (CD146) stimulates the tyrosine phosphorylation of focal adhesion kinase p125(FAK). *J Biol Chem*. 1998;273:26852–26856. doi: 10.1074/jbc.273.41.26852
55. Barron L, Gharib SA, Duffield JS. Lung pericytes and resident fibroblasts: busy multitaskers. *Am J Pathol*. 2016;186:2519–2531. doi: 10.1016/j.ajpath.2016.07.004
56. Alarcon-Martinez L, Yilmaz-Ozcan S, Yemisci M, Schallek J, Kilic K, Can A, Di Polo A, Dalkara T. Capillary pericytes express alpha-smooth muscle actin, which requires prevention of filamentous-actin depolymerization for detection. *Elife*. 2018 Mar 21;7:e34861. doi: 10.7554/eLife.34861
57. Verbeek MM, Otte-Holler I, Wesseling P, Ruiter DJ, de Waal RM. Induction of alpha-smooth muscle actin expression in cultured human brain pericytes by transforming growth factor-beta 1. *Am J Pathol*. 1994;144:372–382.
58. Desmoulière A, Geinoz A, Gabbiani F, Gabbiani G. Transforming growth factor-beta 1 induces alpha-smooth muscle actin expression in granulation tissue myofibroblasts and in quiescent and growing cultured fibroblasts. *J Cell Biol*. 1993;122:103–111. doi: 10.1083/jcb.122.1.103
59. Hinz B. Myofibroblasts. *Exp Eye Res*. 2016;142:56–70. doi: 10.1016/j.exer.2015.07.009
60. Zhao G, Joca HC, Lederer WJ. Dynamic measurement and imaging of capillaries, arterioles, and pericytes in mouse heart. *J Vis Exp*. 2020. doi: 10.3791/61566
61. Birbrair A, Zhang T, Wang ZM, Messi ML, Enikolopov GN, Mintz A, Delbono O. Skeletal muscle pericyte subtypes differ in their differentiation potential. *Stem Cell Res*. 2013;10:67–84. doi: 10.1016/j.scr.2012.09.003
62. Birbrair A, Zhang T, Files DC, Mannava S, Smith T, Wang ZM, Messi ML, Mintz A, Delbono O. Type-1 pericytes accumulate after tissue injury and produce collagen in an organ-dependent manner. *Stem Cell Res Ther*. 2014;5:122. doi: 10.1186/scrt512
63. Horiuchi K, Kano K, Minoshima A, Hayasaka T, Yamauchi A, Tatsukawa T, Matsuo R, Yoshida Y, Tomita Y, Kabara M, et al. Pericyte-specific deletion of ninjurin-1 induces fragile vasa vasorum formation and enhances intimal hyperplasia of injured vasculature. *Am J Physiol Heart Circ Physiol*. 2021;320:H2438–H2447. doi: 10.1152/ajpheart.00931.2020
64. Muhl L, Genové G, Leptidis S, Liu J, He L, Mocci G, Sun Y, Gustafsson S, Buyandelger B, Chivukula IV, et al. Single-cell analysis uncovers fibroblast heterogeneity and criteria for fibroblast and mural cell identification and discrimination. *Nat Commun*. 2020;11:3953. doi: 10.1038/s41467-020-17740-1

65. Su H, Zeng H, Liu B, Chen JX. Sirtuin 3 is essential for hypertension-induced cardiac fibrosis via mediating pericyte transition. *J Cell Mol Med*. 2020;24:8057–8068. doi: 10.1111/jcmm.15437
66. Kramann R, Schneider RK, DiRocco DP, Machado F, Fleig S, Bondzie PA, Henderson JM, Ebert BL, Humphreys BD. Perivascular Gli1+ progenitors are key contributors to injury-induced organ fibrosis. *Cell Stem Cell*. 2015;16:51–66. doi: 10.1016/j.stem.2014.11.004
67. Alvino VV, Fernández-Jiménez R, Rodriguez-Arabaolaza I, Slater S, Mangialardi G, Avolio E, Spencer H, Culliford L, Hassan S, Sueiro Ballesteros L, et al. Transplantation of allogeneic pericytes improves myocardial vascularization and reduces interstitial fibrosis in a swine model of reperfused acute myocardial infarction. *J Am Heart Assoc*. 2018;7:e006727. doi: 10.1161/JAHA.117.006727
68. Avolio E, Meloni M, Spencer HL, Riu F, Katare R, Mangialardi G, Oikawa A, Rodriguez-Arabaolaza I, Dang Z, Mitchell K, et al. Combined intramyocardial delivery of human pericytes and cardiac stem cells additively improves the healing of mouse infarcted hearts through stimulation of vascular and muscular repair. *Circ Res*. 2015;116:e81–e94. doi: 10.1161/CIRCRESAHA.115.306146

SUPPLEMENTAL MATERIAL

Figure S1. Isotype-matched controls demonstrate the specificity of fibroblast and pericyte labeling in dual reporter and lineage tracing systems.

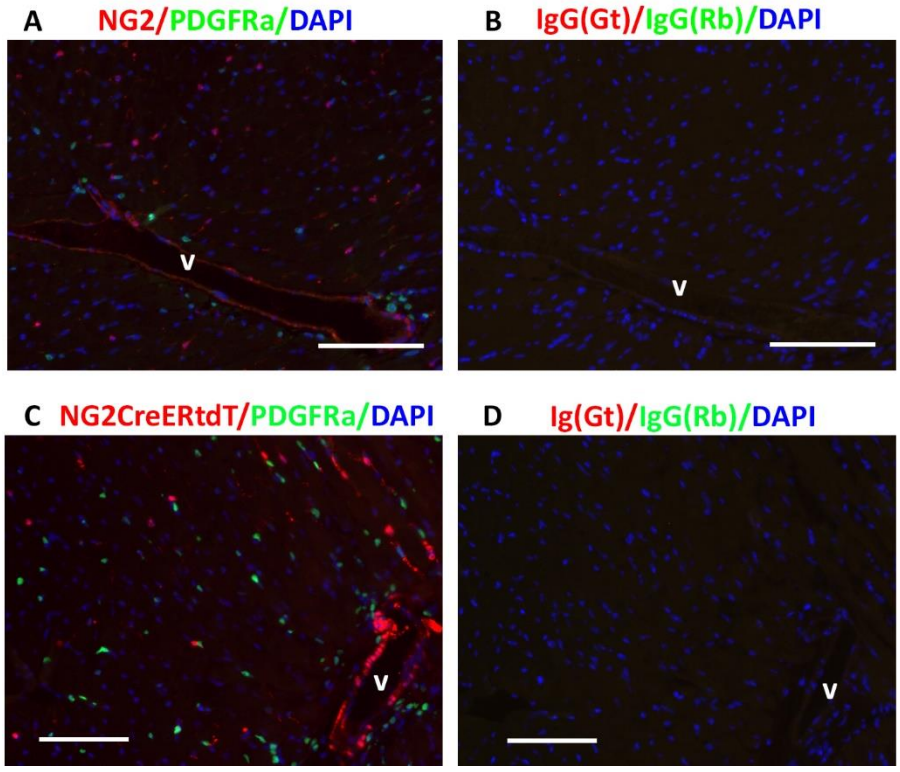

A-B: In myocardial sections from dual reporter NG2^{Dsred};PDGFRα^{EGFP} mice, NG2 labels mural cells (red), whereas PDGFRα stains the nuclei of fibroblasts (green). Isotype-matched controls in a serial section (B) show no staining, demonstrating the specificity of the strategy. Scalebar=80μm. C-D: In a similar manner, isotype-matched controls show the specificity of the lineage tracing approach in PDGRβ$^{iCre/+}$;R26^{tdTomato};PDGFRα^{EGFP} mice. NG2-traced cells appear red, whereas the nuclei of PDGFRα+ fibroblasts are green. An isotype matched control-stained serial section shows no staining. Scalebar=70μm; v, vessel.

Figure S2. Isotype matched controls show the specificity of NG2(Dsred)/PDGFRβ dual immunofluorescence.

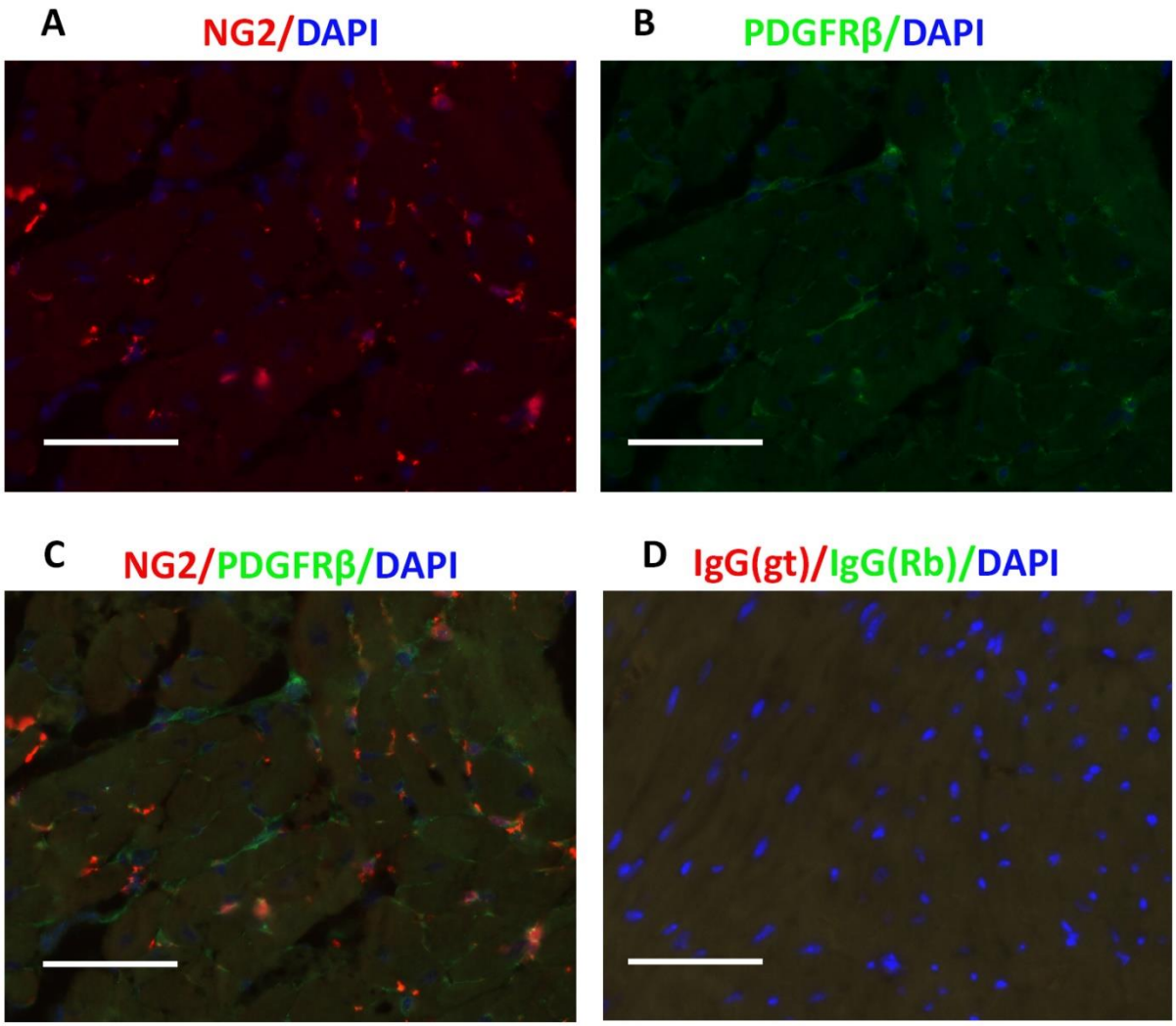

NG2+ positive profiles (red, A) and PDGFRβ-expressing cells (green, B) are identified in the myocardium of $NG2^{Dsred}$ reporter animals. Panel C shows the merged image. D. A section staining with isotype-matched control IgG shows no staining. Scalebar=50μm

Figure S3. Outline of the experimental procedure used to obtain a single cell suspension from dual reporter NG2^{DsRed};PDGFRα^{EGFP} adult mouse heart.

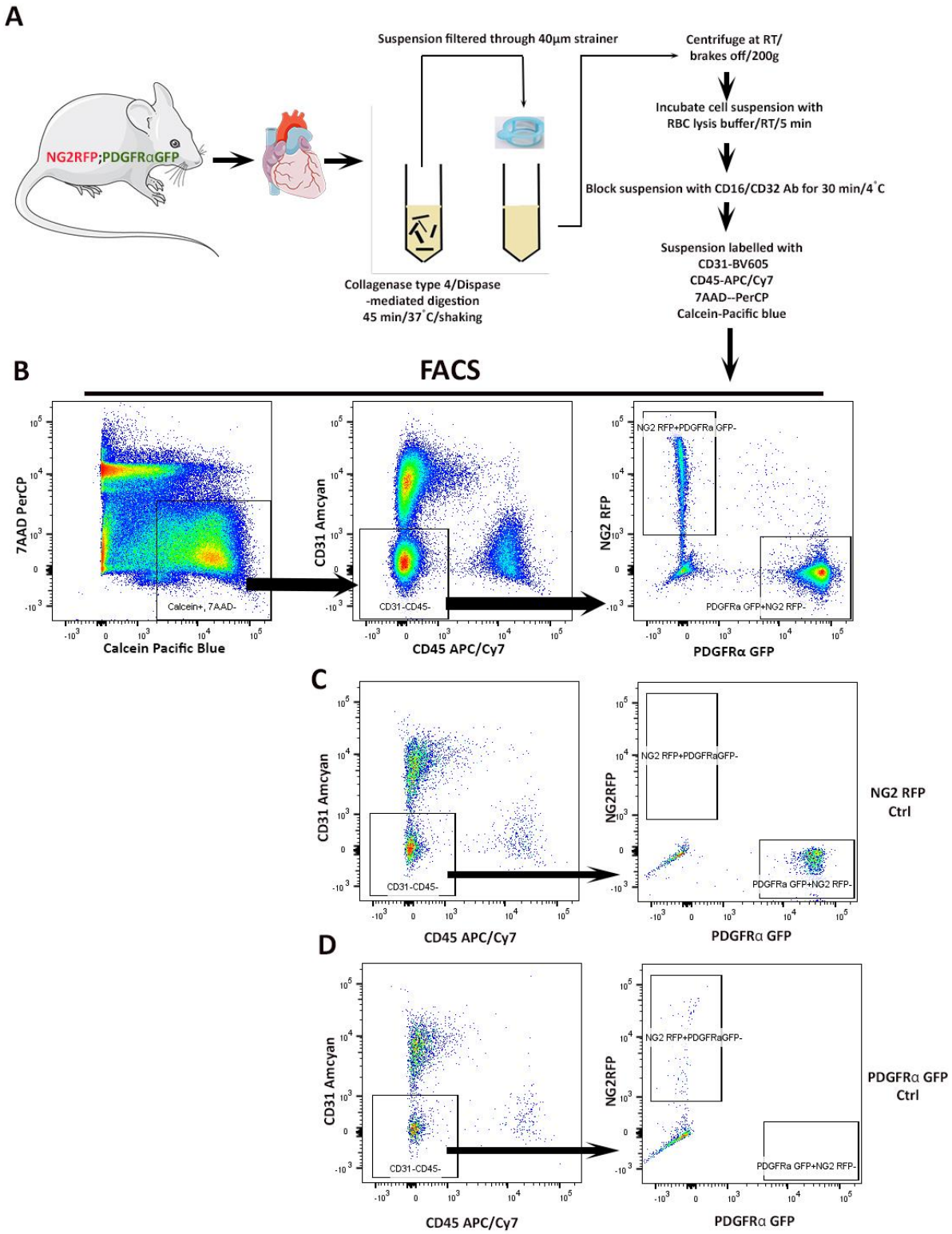

Viable (7AAD-) and metabolically active (calcein+) cells were gated and based on the expression of CD31 and CD45, the non-endothelial and non-hematopoietic cell population was identified. NG2+ and PDGFRα+ populations, subgated from the CD31-CD45- fraction, were FACS-sorted into cell lysis buffer to isolate RNA. C & D. $NG2^{DsRed}$ and $PDGFR\alpha^{EGFP}$ are genetic tags and are identified without the use of antibodies. C represents absence of $NG2^{DsRed}$ population when prepared from $PDGFR\alpha^{EGFP}$ single reporter mouse and D represents the absence of $PDGFR\alpha^{EGFP}$ population when prepared from $NG2^{DsRed}$ mouse model.

Figure S4. NG2+ pericytes and PDGFRα+ fibroblasts exhibit distinct transcriptomic profiles.

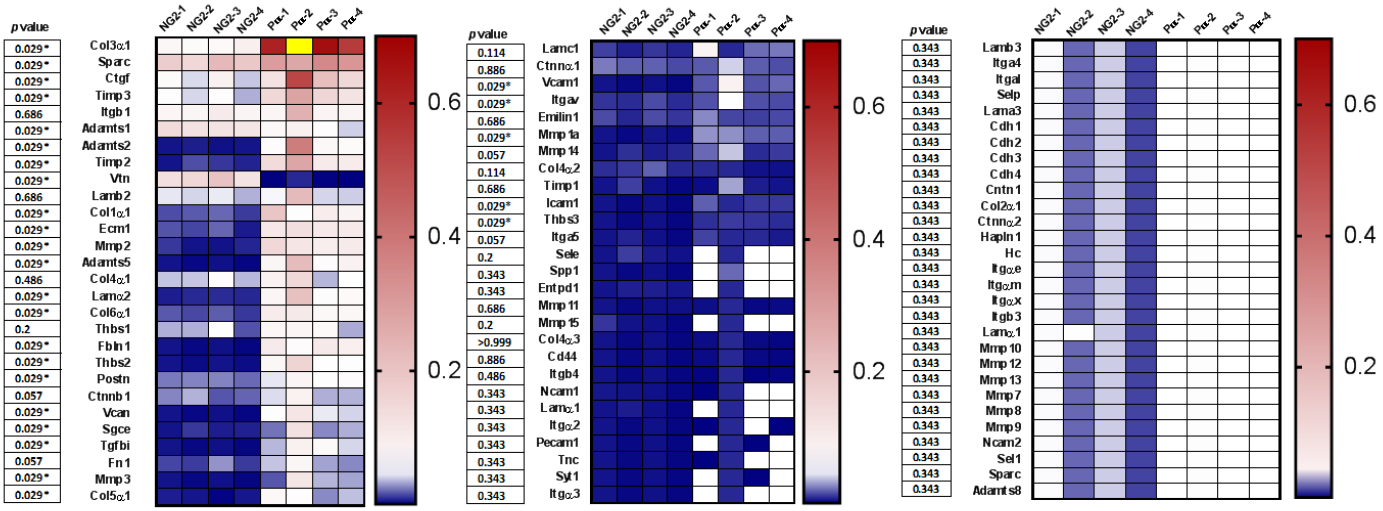

Heat map summarizes the qPCR array data, illustrating differential gene expression of NG2+ pericytes and PDGFRα+ fibroblasts sorted from adult mouse myocardium at baseline and the corresponding p value for each gene (n=4). The sample highlighted in yellow had a very high normalized gene expression value (1.17), that was outside the set range. Statistical comparison was performed using unpaired t-test (for normal distributions), or the Mann-Whitney test for non-Gaussian distributions.

Figure S5. The germline NG2-Cre driver does not specifically label myocardial mural cells.

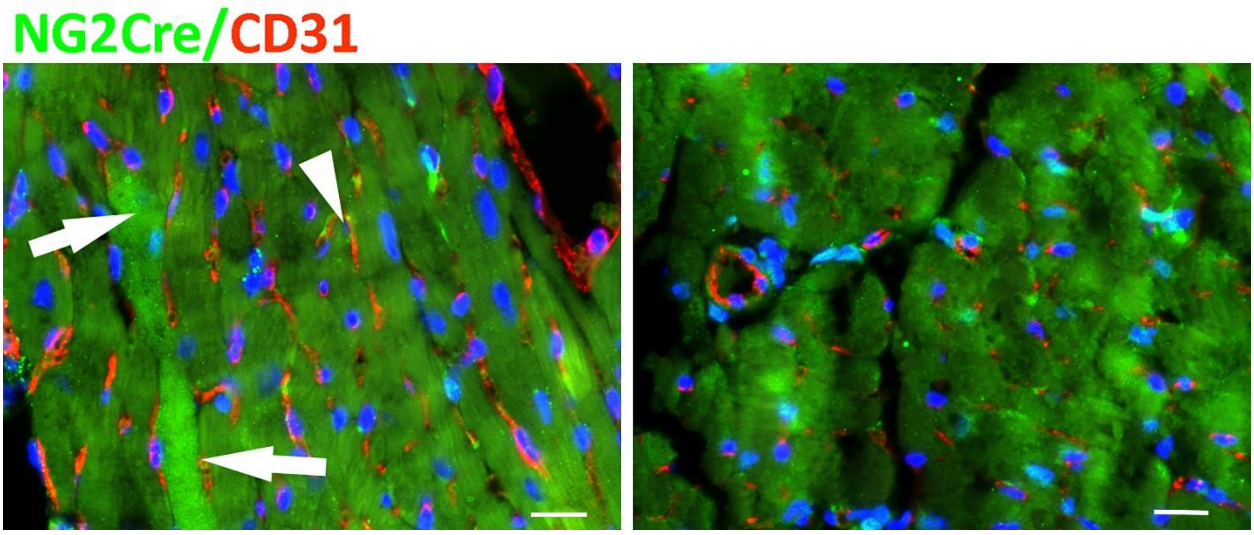

$NG2^{Cre/+};R26^{EYFP}$ mice were generated to trace NG2-derived cells. Dual fluorescence in myocardial sections for EYFP and the endothelial cell marker CD31 (arrrowheads) showed that vascular mural cells could not be specifically identified due to the intense fluorescence in cardiomyocytes (arrows). Images are representative of 6 different experiments. Scalebar=20μm

Figure S6. Labeling of valvular and aortic cells using the inducible NG2CreER^{TM} driver.

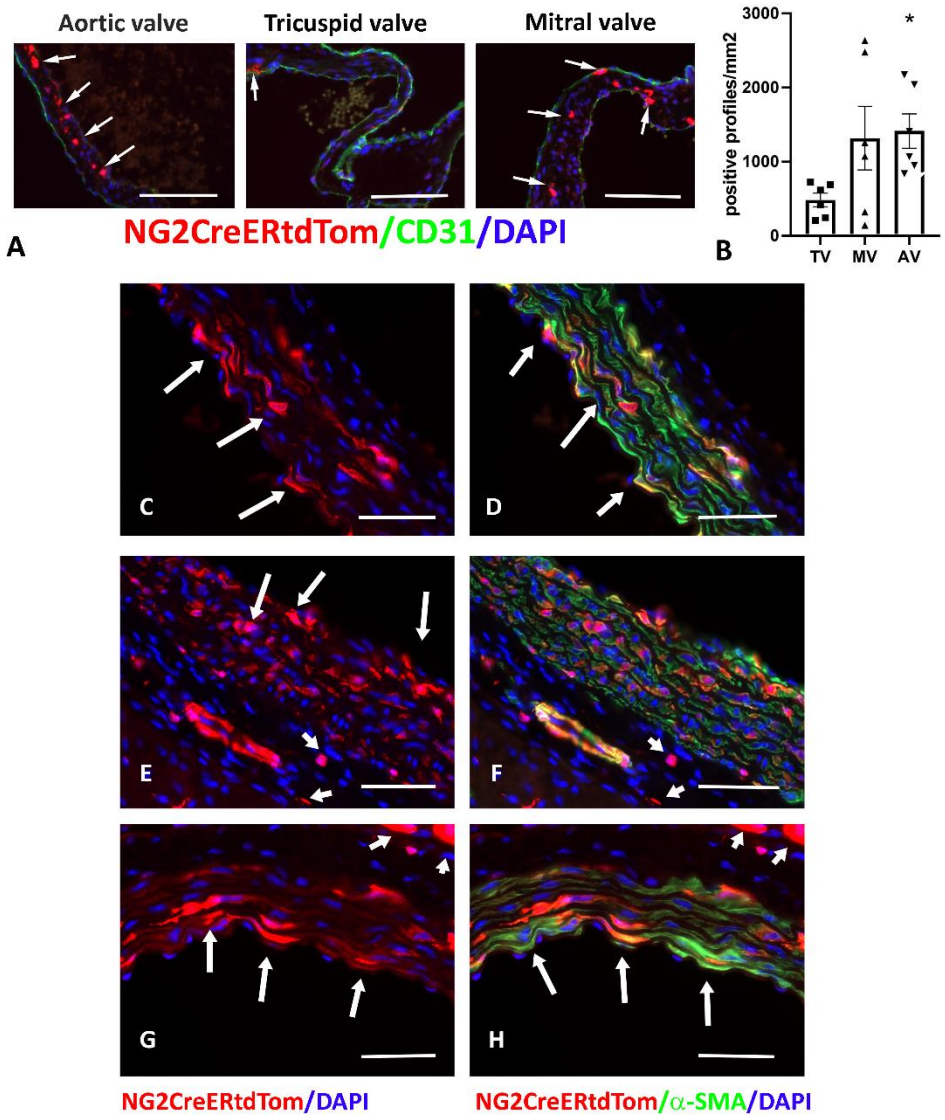

A-B, TdTomato staining of myocardial sections in the NG2CreER^{TM} model labeled a significant population of valvular cells, which were more abundant in the aortic valve (AV). **C-H**, Dual fluorescence for a-SMA and tdTomato shows labeling of mural cells in sections from the ascending aorta. ~60% of aortic medial α-SMA+ vascular smooth muscle cells were labeled with the inducible NG2 Cre driver (long arrows). Occasional α-SMA-negative NG2-labeled adventitial cells may represent pericytes of the adventitial vasa vasorum (short arrows). Images are representative of 6 different experiments. Scalebar=100μm. Data are presented as mean $\pm$ SE. Statistical comparison was performed using non-parametric ANOVA (Kruskall-Wallis).

Figure S7. The inducible PDGFRβCreER^{T2} driver labels abundant valvular cells and a large population of aortic adventitial cells.

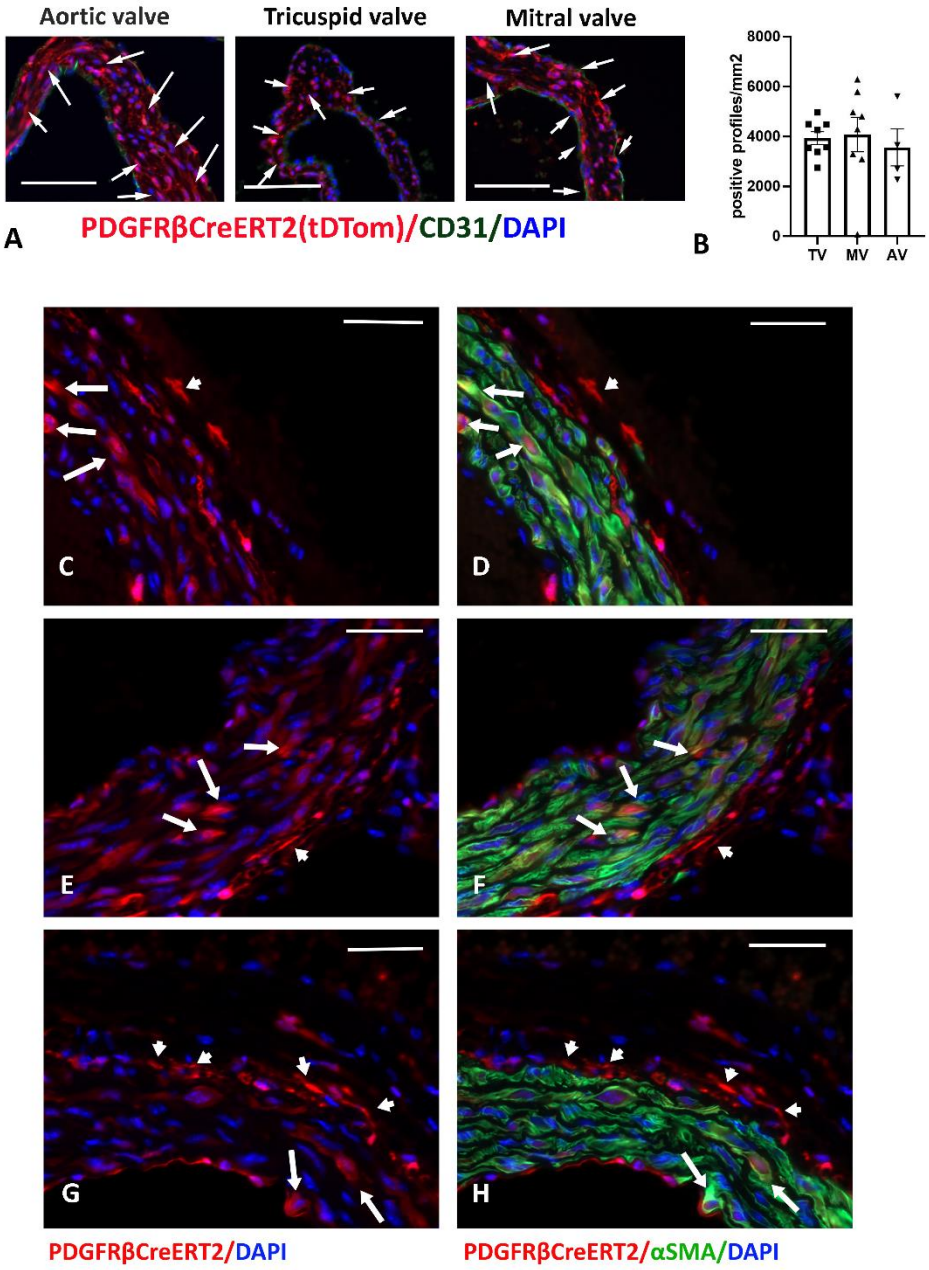

A-B, tdTomato staining in PDGFRβCre^{ERT2} model labeled a much larger population of valvular interstitial cells when compared to the NG2CreER^{TM} model (shown in Suppl Fig VI). **C-H**, Staining of aortic sections showed that ~70% of aortic αSMA+ vascular smooth muscle cells were labeled using the PDGFRβCre^{ERT2} line (long arrows). Moreover, the inducible PDGFRβ Cre driver also labeled a large population of adventitial aortic cells that were negative for α-SMA (short arrows). These cells had morphological characteristics of fibroblasts. Images are representative of 6 different experiments. Scalebar=100μm. Data are presented as mean ± SE. Statistical comparison was performed using non-parametric ANOVA (Kruskall-Wallis).